Central Lancashire Online Knowledge (CLoK)

Title	Integration of JAK/STAT receptor-ligand trafficking, signalling and gene expression in Drosophila melanogaster cells
Type	Article
URL	https://clok.uclan.ac.uk/34837/
DOI	https://doi.org/10.1242/jcs.246199
Date	2020
Citation	Moore, Rachel, Vogt, Katja orcid iconORCID: 0000-0002-4938-563X, Acosta Martin, Adelina E., Shire, Patrick, Zeidler, Martin and Smythe, Elizabeth (2020) Integration of JAK/STAT receptor-ligand trafficking, signalling and gene expression in Drosophila melanogaster cells. Journal of Cell Science, 133 (19). ISSN 0021-9533
Creators	Moore, Rachel, Vogt, Katja, Acosta Martin, Adelina E., Shire, Patrick, Zeidler, Martin and Smythe, Elizabeth

It is advisable to refer to the publisher's version if you intend to cite from the work.
https://doi.org/10.1242/jcs.246199

For information about Research at UCLan please go to http://www.uclan.ac.uk/research/

1   **Integration of JAK/STAT receptor-ligand trafficking, signalling and gene**

2   **expression in *Drosophila melanogaster* cells**

3   Rachel Moore[1,], Katja Vogt[1,2], Adelina E. Acosta Martin[3], Patrick Shire[1], Martin

4   Zeidler[1] and Elizabeth Smythe[1]

5

6   [1.] Centre for Membrane Interactions and Dynamics

7   Department of Biomedical Science

8   University of Sheffield

9   Sheffield

10 S10 2TN

11

12

13 Current address

14 [2.] School of Medicine,

15 University of Central Lancaster,

16 Preston

17 PR1 2HE

18

19 [3.] biOMICS Facility

20 Faculty of Science Mass Spectrometry Centre

21 University of Sheffield

22 Sheffield

23 S10 2TN

24

25

26 Correspondence to: e.smythe@sheffield.ac.uk

27

28 **Running title:** Compartmentalised signalling regulates expression of JAK/STAT

29 targets

30

31

32   **Abstract**
33   The JAK/STAT pathway is an essential signalling cascade required for multiple
34   processes during development and for adult homeostasis. A key question in
35   understanding this pathway is how it is regulated in different cell contexts. Here we
36   have examined how endocytic processing contributes to signalling by the single
37   cytokine receptor, Domeless, in *Drosophila melanogaster* cells. We identify an
38   evolutionarily conserved di-Leu motif that is required for Domeless internalisation and
39   show that endocytosis is required for activation of a subset of Domeless targets. Our
40   data indicate that endocytosis both qualitatively and quantitatively regulates
41   Domeless signalling. STAT92E, the single STAT transcription factor in *Drosophila*,
42   appears to be the target of endocytic regulation and our studies show that
43   phosphorylation of STAT92E on Tyr704, while necessary, is not always sufficient for
44   target transcription. Finally, we identify a conserved residue, Thr702, which is
45   essential for Tyr704 phosphorylation. Taken together, our findings identify previously
46   unknown aspects of JAK/STAT pathway regulation likely to play key roles in the
47   spatial and temporal regulation of signalling *in vivo*.
48

Introduction

50 The Janus Kinase/Signal transducer and activator of transcription (JAK/STAT)

51 signalling pathway regulates a variety of cellular events, including proliferation and

52 apoptosis, throughout development and in adult life (Villarino et al., 2017). According

53 to the canonical model, JAK/STAT signalling involves the activation of homo- or

54 hetero-dimerised cell-surface transmembrane receptors by ligands, including

55 cytokines, growth factors and hormones, which causes a conformational change in

56 the cytoplasmic tail of the receptor. This stimulates activation of the Janus kinases

57 (JAKs) that are constitutively associated with the receptor. JAK activation leads to

58 specific Tyr phosphorylation of both the kinase and the receptor, subsequently

59 allowing recruitment of signal transducer and activator of transcription (STAT)

60 transcription factors through Src-homology 2 (SH2) domains. This association in turn

61 allows JAK to phosphorylate STATs at a highly conserved C-terminal Tyr residue,

62 leading to STAT dimerization and translocation to the nucleus. Here STATs bind to

63 palindromic DNA sequences to alter expression of target genes, resulting in

64 developmental, haematological and immune-related responses (O'Shea et al., 2015;

65 Stark and Darnell, 2012). Dysregulation of the JAK/STAT pathway is involved in the

66 pathogenesis of diseases such as gigantism, asthma, myocardial hypertrophy,

67 myeloproliferative neoplasia and severe combined immunodeficiency (O'Shea et al.,

68 2015).

69

70 The JAK/STAT pathway has been highly conserved through evolution, with

71 invertebrates such as *Drosophila melanogaster* having a full complement of pathway

72 components. However, while mammals have multiple copies of receptors, JAKs and

73 STATs, in *Drosophila* the signalling pathway is composed of a single positively acting

74 receptor, Domeless (Dome) (Brown et al., 2001), a negatively acting receptor, Latran

75 (Makki et al., 2010), one JAK, Hopscotch (Hop), and one STAT, STAT92E (Hou et al.,

76 1996; Yan et al., 1996; Zeidler and Bausek, 2013). Therefore, *Drosophila* provides

77 an excellent model in which to investigate JAK/STAT pathway regulation, without the

78 difficulties of compensation and signalling crosstalk inherent in mammalian systems.

79 In fact, investigating JAK/STAT signalling in *Drosophila* has led to key breakthroughs

80 in understanding the impact of its dysregulation in human disease (Ekas et al., 2010).

81

82 The repeated use of the JAK/STAT pathway in a variety of contexts begs the

83 question as to how transcriptional outputs are differentially regulated in a cell- and

84 tissue-specific manner. One potential mechanism to explain this diversity of outputs

85 is regulation by endocytosis (Sigismund and Scita, 2018; Villasenor et al., 2016;

86   Weinberg and Puthenveedu, 2019). Activated receptors can be internalised into cells

87   by multiple endocytic pathways of which clathrin mediated endocytosis (CME) is the

88   best characterised. Receptor complexes internalised by CME are clustered into

89   clathrin coated pits. The assembled clathrin lattice is linked to the cytoplasmic

90   domains of transmembrane receptors via adaptor proteins, including the AP2 adaptor

91   complex (Mettlen et al., 2018; Owen et al., 2004). In addition to CME, several clathrin

92   independent (CIE) pathways exist which are important for the uptake of particular

93   cargoes (Mayor et al., 2014). Following internalisation, activated receptors are

94   delivered to the early endosome where they may be recycled or targeted to late

95   endosomes and lysosomes for degradation. The Endosomal Sorting Complexes

96   Required for Transport (ESCRT) protein complexes are key for sorting receptors into

97   late endosomes and lysosomes. Hrs is a component of ESCRT-0, acting as an

98   adaptor to select ubiquitinated cargo for targetting to lysosomes. TSG101 is a

99   component of ESCRT I complexes which recruit other ESCRT complexes, which are

100 key in allowing the inward invaginations of the late endosome to form intraluminal

101 vesicles (Henne et al., 2013). Results from *in vivo* and *in vitro* experiments indicate

102 that endocytosis can regulate receptor signalling quantitatively through removal of

103 activated receptors from the cell surface and targeting them to lysosomes for

104 degradation. Endocytosis can also qualitatively regulate signalling by establishing

105 'signalosomes', which are membrane microdomains within endosomal compartments

106 that allow the recruitment of specific scaffolds, adaptors, kinases and phosphatases,

107 thus resulting in different downstream signalling outputs (Carroll and Dunlop, 2017;

108 Lawrence et al., 2019; Moore et al., 2018; Sigismund and Scita, 2018; Villasenor et

109 al., 2016). The route of entry of activated receptors (CME versus CIE) can also

110 influence signaling output as demonstrated for Notch signaling in *Drosophila*

111 (Shimizu et al., 2014) and TGF-beta signaling in mammalian cells (Di Guglielmo et

112 al., 2003). CME is a major entry portal which has been shown to regulate JAK/STAT

113 signalling following activation of several different cytokine receptors in mammalian

114 cells (Cendrowski et al., 2016; Chmiest et al., 2016; German et al., 2011; Kermorgant

115 and Parker, 2008; Marchetti et al., 2006).

116

117 *In vivo* studies in *Drosophila* suggested that Dome-dependent border cell migration

118 requires ligand-dependent CME and delivery to multivesicular bodies (Devergne et

119 al., 2007). Mutation of endocytic components including clathrin heavy chain (CHC),

120 prevented Dome internalisation, decreased STAT92E expression and nuclear

121 translocation in follicle cells. In contrast, endocytosis appeared to negatively regulate

122 JAK/STAT signalling in *Drosophila* Kc_{167} cells (Müller et al., 2008; Vidal et al., 2010).

These varying results likely reflect differences due to cell context as has been observed for endocytic regulation of receptor tyrosine kinases such as epidermal growth factor receptor (EGFR) (Sousa et al., 2012; Vieira et al., 1996; Villasenor et al., 2015). The underlying regulatory mechanisms of context-dependent signalling are however largely unknown.

Canonical signalling by STAT requires phosphorylation at a conserved Tyr (704 in *Drosophila* STAT92E, isoform C used in this study), which allows for parallel dimerization of STATs via their SH2 domains and translocation into the nucleus. There is also evidence that other posttranslational modifications, in addition to phosphorylation of the conserved Tyr, regulate STAT activity (Chung et al., 1997; Costa-Pereira et al., 2011; Gronholm et al. 2010; Karsten et al., 2006; Wang et al., 2005).

Here we show that in *Drosophila* S2R+ cells, endocytosis is essential for the expression of some, but not all, JAK/STAT pathway target genes. We demonstrate that STAT92E is the target for endocytic regulation and, importantly, that endocytosis qualitatively regulates STAT92E activity. In addition, we have identified a novel phosphorylation site Thr702, which is crucial for Tyr704 phosphorylation of STAT92E.

Results

Dome internalisation requires an evolutionarily conserved di-Leu cassette

To understand mechanisms of Dome internalisation, we first asked how Dome and its ligand Upd2 are taken into cells. Similar to mammalian cells, *Drosophila* cells can internalise material by a variety of CME and CIE mechanisms (Shimizu et al., 2014). It has been shown that Dome is internalised into *Drosophila* Kc$_{167}$ cells by CME (Müller et al., 2008; Vidal et al., 2010). To investigate if this is the case in S2R+ cells, we measured internalisation of Upd2-GFP, as a proxy for receptor internalisation, using an anti-GFP ELISA assay (Wright et al., 2011). We first treated cells with dsRNA targeting Dome and found that there is a significant reduction in the rate (-38%) and extent (-50%) of uptake of Upd2-GFP at both high (20 nM, Figure 1A) and low (3 nM, Fig. S1A) concentrations of Upd2-GFP. Under these conditions levels of Dome mRNA are reduced by ~90% (Figure S1B). The residual uptake of Upd2-GFP in the absence of Dome is likely due to non-specific fluid phase uptake of ligand. When cells were incubated with 20nM Upd2-GFP, knockdown of CHC and AP2 reduced the uptake of Upd2-GFP by approximately 60% compared to knockdown of Dome alone (Figure 1A). Since levels of CHC and AP2 mRNA were reduced by ~80% following dsRNA knockdown, this suggests that the Upd-2-GFP complex can be internalised by CIE as well as CME, as has been shown for several receptors in mammalian cells (Sigismund et al., 2005; Vander Ark et al., 2018) and for Notch and Delta in *Drosophila* (Shimizu et al., 2014). By contrast, when S2R+ cells were incubated with low concentrations of Upd2-GFP (3 nM), knockdown of CHC reduced the uptake of Upd2-GFP to the level observed following Dome knockdown (Figure S1A). Together this suggests that at low concentrations of Upd2-GFP, Dome is primarily internalised by CME, but that increasing concentrations of ligand results in Dome also being internalised via CIE.

Sorting of cargo into clathrin coated pits requires internalisation motifs in the cytoplasmic tails of receptors that include both Tyr- and di-Leu-based motifs (Traub, 2003). Dome is most similar in sequence and structure to gp130, which is a co-receptor shared by receptors for IL-6 (Figure 1B). Internalisation of gp130 requires a di-Leu motif (^{786}LL^{787}) in its cytoplasmic domain (Dittrich et al., 1996) while an upstream serine within the sequence ^{780}**S**ESTQP**LL**^{787} has also been shown to be important for rapid internalisation (Dittrich et al., 1996). Strikingly, the cytoplasmic tail of Dome also contains a di-Leu motif, ^{985}LL^{986}, in a similar context to that of the di-Leu motif in gp130 (Figure 1C). In order to test the potential significance of this motif, we generated a series of FLAG-tagged Dome mutant constructs where individual

6

181 elements of the di-Leu cassette were mutated either alone or in combination (Figure

182 1C), and transfected these constructs into S2R+ cells. To quantitatively measure

183 ligand dependent uptake of the engineered Dome constructs, proteins on the surface

184 of transfected S2R+ cells were biotinylated prior to addition of Upd2-GFP. This

185 showed that while expression of the mutants was somewhat more efficient than

186 transfection of wild-type Dome (Figure S1C), plasma membrane expression all of the

187 constructs was comparable (Figure S1D). Following ligand internalisation, cell

188 surface biotin was removed by treatment with the reducing agent, 2-

189 mercaptoethanesulfonic acid sodium salt, MESNa, while internalised cell surface

190 proteins were protected and remained biotinylated. This allowed the amount of

191 internalised wild-type and mutant Dome to be quantitated. As has been

192 demonstrated previously for Dome (Ren et al., 2015), we observed ligand-

193 independent internalisation of Dome (Figure S1E). We found that mutation of the

194 entire di-Leu cassette to AAASKAA (defined from now on as Dome^{allA}) inhibited

195 internalisation of Dome. Mutation of the di-Leu motif alone (Dome^{LL985AA}-FLAG) did

196 not significantly reduce internalisation. Using site-directed mutagenesis in which we

197 progressively replaced elements of the putative cassette, we established that Glu980

198 and LL985-6 together represent essential residues required for Dome internalisation

199 (Figure 1D and E). Mutation of Glu980 alone did not significantly affect Dome

200 internalisation (Figure S1F and S1G). Although uptake of Dome $^{E980G/LL985AA}$-FLAG

201 was significantly inhibited (~66%), the effect on internalisation was less than that

202 observed for the Dome^{allA}-FLAG mutant, suggesting that other determinants may

203 also be present within the sequence which are important for Dome internalisation

204 (Figure 1D and 1E). Together these results identify a di-Leu-containing cassette as

205 being essential for Dome internalisation.

206

207 *Dome signalling is regulated by endocytosis*

208 Dome signalling is known to be regulated by endocytosis in Kc$_{167}$ cells (Müller et al.,

209 2008; Vidal et al., 2010) and *in vivo* (Devergne et al., 2007). To test whether it is

210 similarly regulated in S2R+ cells, we measured the expression of the exogenous

211 reporter *10XSTAT-Luciferase,* which expresses the firefly luciferase enzyme under

212 the control of a minimal promoter downstream of ten STAT92E binding sites (Baeg et

213 al., 2005). As expected, this reporter is activated in S2R+ cells by exogenous Upd2-

214 GFP, in a dose dependent manner (Figure 2A), indicating that these cells express

215 the JAK/STAT pathway components required for activation. We next measured

216 Upd2-GFP-dependent *10xSTAT-Luciferase* reporter activity in control cells and those

217 expressing Dome ^{wt}-FLAG or Dome^{allA}-FLAG (Figure 2B). While expression of

218 Dome^{wt}-FLAG did not significantly affect signalling, expression of Dome^{allA}-FLAG had

219 a strong dominant negative effect on Upd2-GFP mediated pathway stimulation. This

220 effect was comparable to the level observed in cells expressing Dome$^{Y966A/Q969A}$-

221 FLAG and Dome^{P925I}-FLAG, mutants which have been previously reported to have

222 reduced signalling because of their inability to bind STAT92E (Stahl and

223 Yancopoulos, 1994) and Hop respectively (Fisher et al., 2016). Levels of expression

224 of the transfected proteins are shown in Figure S2A. Together these data

225 demonstrate that Dome mutants that cannot be internalised, also alter JAK/STAT

226 signalling and are consistent with a model where activation of *10XSTAT-Luciferase*

227 by Upd2-GFP is dependent on Dome internalisation.

228

229 *Endocytosis generates qualitatively different transcriptional outputs.*

230 To further explore a role for endocytosis in regulating signalling downstream of

231 Dome, we asked whether knocking down components of the endocytic machinery

232 might differentially affect expression of Dome target genes. We therefore examined

233 the expression of the *10xSTAT-Luciferase* reporter and the endogenous target genes

234 *socs36E* and *lama* (Flaherty et al., 2009; Karsten et al., 2002) in cells treated with

235 dsRNA to knock down endocytic components. We targeted AP2, an adaptor whose

236 knockdown is predicted to result in accumulation of receptors at the cell surface

237 (Robinson, 2004), Hrs, an adaptor whose knockdown is likely to result in

238 accumulation of ubiquitinated receptors in early endosomes, and TSG101 which is

239 required for the sorting of receptors into intraluminal vesicles and whose knockdown

240 is likely to lead to an accumulation of receptors on the limiting membrane of late

241 endosomes (Henne et al., 2013). Treating cells with dsRNA to knockdown Dome

242 (levels of Dome mRNA were reduced by ~ 90%, Figure S1B) resulted in almost

243 complete abolition of *10XSTAT-Luciferase* expression, demonstrating that both

244 background, and Upd2-GFP-stimulated, reporter activation are receptor-dependent

245 (Figure 2C). In the absence of exogenous ligand, activation of *10XSTAT-Luciferase*

246 in cells treated with dsRNA targeting AP2, Hrs or TSG101, was however unchanged

247 compared to cells treated with control dsRNA (Figure 2C). We speculate that this

248 ligand-independent activation is due to expression of ligands and growth factors that

249 may cross-talk with the JAK/STAT pathway in S2R+ cells (Cherbas et al., 2011). By

250 contrast knockdown of AP2 significantly reduced ligand dependent *10XSTAT-*

251 *Luciferase* activation whereas knockdown of Hrs or TSG101 had no effect. This

252 indicates that activation of this reporter requires delivery of activated Dome either to,

253 or beyond, an AP2-positive endocytic compartment but prior to an Hrs-positive

254 endosomal compartment. We also examined an endogenous target of Dome,

255 *socs36E* (Stec et al., 2013) and found that, in contrast to *10xSTAT-Luciferase*
256 expression, knockdown of both AP2 and Hrs inhibited *socs36E* mRNA expression
257 while knockdown of TSG101 had no effect (Figure 2D). This indicates that activated
258 Dome must be trafficked to an Hrs-positive compartment, or beyond, to allow
259 downstream pathway activation to trigger *socs36E* transcription. Taken together
260 these results indicate that the location of the activated Upd2/Dome complexes within
261 the endocytic pathway can lead to qualitatively different signalling outputs. It is
262 important to note that not all Dome target genes are regulated by endocytosis. For
263 example, expression of *lama*, a well-characterised target of STAT92E (Flaherty et al.,
264 2009), was unaffected when endocytosis was perturbed, suggesting that expression
265 of this target gene mRNA can be driven by activated Upd2:Dome complexes which
266 are located on the plasma membrane (Figure S2B).
267
268 *Phosphorylation of STAT92E is necessary, but not sufficient, for transcription of*
269 *some JAK/STAT targets*
270 Upon ligand activation of Dome, STAT92E is phosphorylated by Hop at a conserved
271 Tyr residue (Y704) (Yan et al., 1996). This residue is conserved across all vertebrate
272 STATs, and its phosphorylation is essential for canonical STAT activity and target
273 expression. We therefore asked whether Tyr704 phosphorylation of STAT92E was
274 sensitive to endocytic regulation. One approach to assaying STAT92E
275 phosphorylation utilizes its change in electrophoretic mobility on SDS-PAGE gels
276 (Shi et al., 2008), caused by changes in charge and conformation that occur
277 following phosphorylation (Mao et al., 2005; Wenta et al., 2008). Using this
278 experimental approach, we observed an Upd2 dose-dependent change in the
279 electrophoretic mobility of STAT92E following ligand stimulation (Figure 3A and B),
280 which was reversed by phosphatase treatment (Figure 3C and D). Strikingly,
281 perturbation of the endocytic pathway, by knockdown of AP2 (Figure 3E and F), or
282 Hrs or TSG101 (Figure S3), did not affect the temporal dynamics of STAT92E
283 phosphorylation, a finding that was also confirmed by mass spectrometry (Figure 3G
284 and Supplemental data 1 and 2, available via ProteomeXchange with identifier
285 PXD020719). These data demonstrate that phosphorylation of Tyr704 on STAT92E
286 is not regulated by endocytosis and that other mechanisms must be responsible for
287 the pathway's sensitivity to endocytic regulation.
288
289 *STAT92E-GFP nuclear import is not affected by knockdown of endocytic*
290 *components*.

291 Canonical JAK/STAT pathway signalling requires nuclear import of the STAT92E

292 transcription factor to activate gene expression. We therefore investigated whether

293 knockdown of AP2 impaired translocation of STAT92E into the nucleus. Nuclear

294 accumulation can be visualized in S2R+ cells transfected with STAT92E-GFP. In the

295 absence of ligand there appears to be low levels of STAT92E-GFP in the nucleus.

296 This is consistent with reports that STATs shuttle between the nucleus and

297 cytoplasm in a phosphorylation-independent manner and that unphosphorylated

298 nuclear STATs can perform non-canonical functions (Brown and Zeidler, 2008). The

299 levels of nuclear STAT92E-GFP we observe in the absence of Upd2 is also in

300 keeping with reports of GFP-tagged proteins entering the nucleus independently of a

301 nuclear localisation signal (Seibel et al., 2007). When cells are treated with Upd2-

302 GFP (Figure 4A and B), a maximum accumulation is reached after 30 minutes

303 stimulation. This is comparable to the nuclear accumulation of mammalian STATs

304 (McBride et al., 2000) and the time-point at which STAT92E phosphorylation is

305 maximal (data not shown). Consistent with previous studies (Begitt et al., 2000;

306 Schindler et al., 1992), mutation of STAT92E Tyr704 (Y704F) to prevent

307 phosphorylation, abolished nuclear accumulation (Figure 4C). While knockdown of

308 Dome almost completely abolished nuclear accumulation of STAT92E-GFP,

309 knockdown of either AP2 or Hrs had no significant effect, indicating that endocytic

310 trafficking of Upd2/Dome does not regulate nuclear accumulation of STAT92E

311 (Figure 4D). This demonstrates that the loss of target gene expression following AP2

312 and Hrs knockdown is not likely to be the result of a defect in the translocation of

313 STAT92E into the nucleus.

314

315 *Thr702 phosphorylation is essential for STAT92E activity*

316 Given that Y704 phosphorylation is necessary but not sufficient for STAT92E-driven

317 pathway gene expression, we wanted to investigate whether other post-translational

318 modifications of STAT92E might be associated with pathway activation. We

319 expressed STAT92E-GFP in S2R+ cells, stimulated with Upd2-GFP, and subjected

320 samples, isolated using GFP-TRAP beads, to mass spectrometry analysis. In

321 addition to Tyr704, this analysis identified Thr47, Ser227 (Figure 5A, Supplemental

322 data 1, 3 and 4, available via ProteomeXchange with identifier PXD020719) and

323 Thr702 (with lower confidence) on STAT92E as being phosphorylated (Supplemental

324 data 1 and 5, available via ProteomeXchange with identifier PXD020719). We

325 therefore decided to test the potential physiological relevance of these newly

326 identified phosphorylation sites using an S2R+ cell line lacking endogenous

327 STAT92E. We used CRISPr/Cas9 to engineer STAT92E negative S2R+ cells,

328   demonstrating that the cell line no longer had detectable STAT92E by Western

329   blotting (Figure S4A) and T7 endonuclease assay (Figure S4B) and was no longer

330   able to activate *10xSTAT-Luciferase* in response to Upd2-GFP (Figure 5B). As

331   expected, expression of wild type STAT92E was able to rescue both Upd2-GFP-

332   dependent and -independent *10XSTAT-Luciferase* activity (Figure S4C) in these

333   STAT92E negative cells, while ligand dependent *10XSTAT-Luciferase* activity was

334   further enhanced by expression of STAT92E^{K187R}, a mutant form of STAT92E which

335   cannot be SUMOylated and which has previously been shown to increase Luciferase

336   activity (Gronholm et al., 2010). Taken together, these results demonstrate the utility

337   of the STAT92E negative S2R+ cells for rescue experiments (Figure S4C).

338

339   We next generated mutant forms of STAT92E lacking both known, and candidate,

340   phosphorylation sites (T47V, S227A, T702V and Y704F), and expressed them in

341   STAT92E negative S2R+ cells and measured their ability to activate *10xSTAT-

342   Luciferase*. Following ligand stimulation with 0.75nM Upd2-GFP, STAT92E^{T47V}

343   STAT92E^{S227A} and STAT92E^{WT} resulted in comparable levels of *10xSTAT-Luciferase*

344   while STAT92E^{T702V} and STAT92E^{Y704F} showed no activation (Figure 5C). This

345   indicates that phosphorylation of Thr702 as well as Tyr704, but not Thr47 or Ser227,

346   is required for JAK/STAT signalling.

347

348   *Phosphomimetic forms of STAT92E rescue signalling*

349   To further explore the role of Thr702 phosphorylation in STAT92E mediated gene

350   activation, we generated phosphomimetics of Thr702 (STAT92E^{T702D}, STAT92E^{T702E})

351   and tested their effects on the *10xSTAT-Luciferase* reporter. Using the STAT92E

352   negative S2R+ cell assays, we first showed that expression of 'loss-of-

353   phosphorylation' mutants STAT92E^{T702V} and STAT92E^{Y704F} did not stimulate reporter

354   activity above background levels (Figure 5D). By contrast, expression of both

355   phosphomimetics STAT92E^{T702D} and STAT92E^{T702E} were sufficient to increase both

356   ligand-dependent and ligand-independent *10xSTAT-Luciferase* expression, with

357   STAT92E^{T702D} more effective in both cases. Taken together, we have thus identified a

358   novel posttranslational modification of STAT92E which is essential to trigger

359   transcriptional activity in this assay.

360

361   *Phosphorylation of Thr702 is required for Tyr704 phosphorylation*

362   We next asked whether Thr702 phosphorylation is required for nuclear translocation

363   of STAT92E and found that Upd2-GFP does not stimulate STAT92E^{T702V}

364   translocation into the nucleus (Figure 6A and B). Using mass spectrometry, we found

11

365   that STAT92E^{T702V} showed a substantial reduction in Tyr704 phosphorylation (Figure

366   6C, Supplemental Data 1 and 6, available via ProteomeXchange with identifier

367   PXD020719). This indicates that phosphorylation of Thr702 is essential for efficient

368   phosphorylation of Tyr704 which, in turn, is essential for the bulk of canonical

369   JAK/STAT gene expression.

370

Discussion

In this work we have explored regulatory mechanisms of JAK/STAT signalling following Upd2-dependent Dome activation in *Drosophila* S2R+ cells. We have identified an evolutionarily conserved internalisation motif in the cytoplasmic tail of Dome. We have demonstrated that internalisation and endocytic trafficking of activated Dome allows for compartmentalised signalling to regulate subsets of *Drosophila* JAK/STAT transcriptional targets, through a mechanism that is independent of Tyr704 phosphorylation of STAT92E. We have also demonstrated that phosphorylation of Thr702 is essential for Tyr704 phosphorylation of STAT92E, its translocation to the nucleus and its activity as a transcription factor.

It has been shown that Dome enters cells by CME *in vivo* in *Drosophila* (Devergne et al., 2007) and *in vitro* in Kc$_{167}$ cells (Müller et al., 2008; Vidal et al., 2010). Our results also support a role for CME in Dome uptake in S2R+ cells since dsRNA mediated knockdown of CHC and AP2 reduce Upd2-GFP internalisation. There are a number of defined motifs that allow the inclusion of transmembrane receptors into clathrin coated pits, through interactions with adaptor molecules such as AP2. A di-Leu motif is one such motif, which is well documented to bind to the α-σ2 hemicomplex of AP2 (Doray et al., 2007; Kelly et al., 2008). In this work we have demonstrated that such a motif is part of a cassette, which is essential for efficient internalisation of Dome. Interestingly, a di-Leu-containing cassette is also required for the internalisation of gp130, the closest vertebrate homologue of Dome and the co-receptor for IL-6R, which is necessary for IL-6R internalisation (Dittrich et al., 1996). Similar to gp130, mutation of the di-Leu motif alone in Dome was insufficient to completely abolish internalisation. In the case of gp130, a Ser upstream of the di-Leu motif was also shown to be involved in rapid internalisation. We found that mutation of the equivalent Ser, in combination with mutation of the di-Leu motif, further reduced Dome internalisation although still not to the same extent as in the Dome^{allA} mutant. An acidic residue (Glu or Asp) at -4 position is commonly found adjacent to di-Leu motifs, and its mutation has previously been shown to drastically decrease binding to the α- σ2 hemicomplex of AP2 (Doray et al., 2007). Mutation of this charged residue alone had no effect on receptor internalisation, while mutation of both the Glu and di-Leu reduced internalisation by approximately 66% compared to Dome^{wt}. This suggests that while the Glu and di-Leu are important, other residues may also influence Dome internalisation. It also points to an important evolutionary conservation in mechanisms of Dome internalisation in line with the conservation of JAK/STAT pathway components across species.

408

Our results support a role for CIE, in addition to CME, in uptake of activated Dome in
S2R+ cells. While dsRNA-mediated knockdown of CHC and AP2 inhibits
internalisation of Upd2-GFP/Dome, the extent of inhibition depends on the
concentration of the Upd2-GFP ligand. At low concentrations (3 nM) of Upd2-GFP,
there is an absolute requirement for CHC and AP2, whereas at higher concentrations
(20 nM), uptake of Upd2-GFP/Dome in cells treated with dsRNA targeting CHC and
AP2 is inhibited by approximately 50% compared to cells treated with dsRNA
targeting Dome. This is consistent with studies in *Drosophila* where uptake of Notch
and Delta through different endocytic pathways (CME and CIE) leads to delivery to
different endosomal compartments and differential signalling and the balance of flux
between these pathways allows cells to respond to different environmental conditions
(Shimizu et al., 2014). Similarly, in mammalian cells, activated receptor tyrosine
kinases such as TGF-beta receptors and EGFR can be taken up by CME and CIE,
with CME being favoured at lower ligand concentrations (Di Guglielmo et al., 2003;
Sigismund et al., 2005). As with Notch signalling, the route of entry of the receptors
can determine signalling outcome and receptor fate (Sigismund et al., 2013; Vander
Ark et al., 2018). The concept of endocytosis modulating Dome target gene
expression in different cells and tissues is supported by previous *in vitro* and *in vivo*
studies (Devergne et al., 2007l; Silver et al., 2005; Vidal et al., 2010). Our
experiments, which have focussed on CME of activated Dome, indicate that
endocytosis also regulates a subset of Dome signalling in S2R+ cells. Mutation of the
internalisation motif not only prevents Dome uptake but also prevents Dome
activation of *10XSTAT-Luciferase,* consistent with a role for endocytosis in activation
of target genes. It is noteworthy that we observe constitutive internalisation and
recycling of Dome in the absence of ligand, as has been observed, in mammalian
cells, for other cytokine receptors (Thiel et al., 1998). Regulation of constitutive
recycling provides cells with a mechanism to control cell surface levels of receptor,
which in turn will impact on the magnitude of signalling (Moore et al., 2018).

Strikingly, we have demonstrated that endocytosis of Dome allows an additional level
of regulatory control in that delivery to distinct endosomal populations can further
affect signalling outcome. Endocytosis is not required for expression of all genes, e.g.
lama, which is still expressed even when components of the endocytic machinery are
ablated with dsRNA. By contrast, expression of *10XSTAT-Luciferase* requires
delivery to, or beyond, an AP2-positive compartment, and expression of *socs36E*
only occurs when activated Dome has trafficked through an Hrs-positive

445 compartment, but before it has reached a TSG101-positive compartment (Figure 6D).

446 Our data thus demonstrate that qualitatively different signalling outputs can occur

447 depending on the location of the activated receptor within the endocytic pathway.

448 This strongly supports the concept that the rate at which receptors, in this case

449 Dome, move through the pathway (endocytic flux) is key for signalling outputs and

450 will have profound effects on downstream cell behaviours. This is consistent with

451 studies on EGFR signalling which imply that receptor signalling can modulate the

452 endocytic machinery to determine the rate of receptor flux (Villasenor et al., 2015).

453 Although mechanistic details for endocytic regulation of signalling are better

454 understood for RTKs and GPCRs, there is a considerable body of emerging

455 evidence to support a role for endocytic regulation of cytokine receptors in

456 mammalian cells (Cendrowski et al., 2016). Our data are thus consistent with a

457 variety of studies in mammalian cells demonstrating an instructive role for

458 endocytosis in JAK/STAT signalling (Cendrowski et al., 2016; Chmiest et al., 2016;

459 German et al., 2011; Kermorgant and Parker, 2008; Marchetti et al., 2006).

460

461 In *Drosophila*, STAT92E is the single transcription factor utilised by the JAK/STAT

462 pathway to control expression of many different target genes, which are expressed in

463 a tissue-specific and developmentally-regulated manner. The essential role of Tyr704

464 phosphorylation in JAK/STAT signalling is well-established (Yan et al., 1996). We

465 eliminated the possibility that endocytosis is required for STAT92E phosphorylation

466 by demonstrating that STAT92E is phosphorylated to the same extent, even when

467 components of the endocytic machinery, such as AP2, are knocked down by dsRNA.

468 More importantly what our data demonstrate is that STAT92E Tyr704

469 phosphorylation, although necessary, is not sufficient for the expression of all Dome

470 target genes. Our data are consistent with previous studies showing that a mutant

471 form of STAT92E, which cannot be methylated is hyper phosphorylated but has a

472 dominant negative effect on target gene expression (Karsten et al., 2006).

473

474 When the endocytic pathway is disrupted, phosphorylated STAT92E can still

475 translocate into the nucleus but it is no longer fully signalling competent. This implies

476 that Dome needs to reach a particular endosomal subcompartment or microdomain

477 in order to allow STAT92E to become transcriptionally competent. Of particular

478 interest is the post-Hrs and pre-TSG101 compartment required for *socs36E*

479 expression (Figure 6D). Hrs is a component of ESCRT-0 complex that recognises

480 ubiquitinated signalling cargo destined to be packaged into inward invaginations of

481 the endosomal membrane to form ILVs and ultimately multivesicular bodies. TSG101

482 is required for later stages of ILV formation (Vietri et al., 2019). As such both these

483 components are found within the same limiting membrane. It has been proposed that

484 membrane microdomains of defined composition, containing signalling molecules,

485 must be able to form within endosomal membranes to generate local signalling

486 competent (signalosome) domains (Shimizu et al., 2014; Teis et al., 2002). Within

487 these specialised signalosomes, STAT92E is likely either to undergo additional

488 posttranslational modifications or to acquire a chaperone protein that facilitates its

489 ability as a transcription factor for a subset of target genes. Support for a Hrs

490 signalosome comes from studies that demonstrate that the Hrs interacting protein

491 STAM is required for downstream signalling following IL2-R activation (Takeshita et

492 al., 1997; Tognon et al., 2014). In mammals, STAMs are phosphorylated in response

493 to a range of cytokines and growth factors (Pandey et al., 2000). The Hrs/STAM

494 complex remains an interesting link between signalling and endocytosis, as it has

495 been shown to have both positive and negative roles in the regulation of RTK

496 signalling in *Drosophila*, which are dependent on the specific tissue and

497 developmental stage (Chanut-Delalande et al., 2010).

498

499 Previous studies in mammalian cells have shown that endosomal location is required

500 for STAT3 activation by activated c-Met which is classed as a weak activator, and it

501 was proposed that by localising STAT3 activation in endosomes, nuclear import is

502 facilitated (Kermorgant and Parker, 2008). Here we show the importance of

503 localisation at different points along the endocytic pathway to nuance Dome

504 signalling to allow different signalling outputs with STAT92E being a target for

505 endocytic regulation.

506

507 Mass spectrometry analysis revealed Thr702 as a novel phosphorylation site on

508 STAT92E that is functionally important. Mutation to Val which is structurally similar

509 but cannot be phosphorylated, prevented STAT92E Tyr704 phosphorylation and

510 nuclear translocation, while phosphomimetic forms of Thr702 rescued this phenotype.

511 Alignment (Waterhouse et al., 2018) of STAT92E with the published crystal structure

512 of STAT1 (Chen et al., 1998) suggests that Thr702 and Tyr704 are located in a

513 flexible loop region (Figure 6E). Phosphorylation is likely to have significant effects

514 on the conformation of this region. Intriguingly this Thr is conserved in STAT1 and is

515 a phosphomimetic in STAT5 suggesting that it may play a role in ensuring effective

516 Tyr phosphorylation of STATs across species.

517

518 *Conclusion*

519   In summary we have shown that endocytosis regulates JAK/STAT signalling in

520   *Drosophila* S2R+ cells resulting in qualitatively different signalling outputs. We

521   therefore suggest that the endocytic flux of activated Dome provides a mechanism by

522   which JAK/STAT can regulate different cellular behaviours depending on cell context.

523   In the course of our studies we have shown that while phosphorylation of Tyr704 on

524   STAT92E is necessary, it is not sufficient for expression of some JAK/STAT target

525   genes. Moreover for some targets, delivery to an endosomal sub-compartment is

526   required in order to make STAT92E transcriptionally competent.

527

528

Methods

Cell culture

S2R+ cells were cultured at 25°C in Schneider's Insect Tissue Culture media (Gibco, UK), supplemented with 10% heat inactivated FBS (Sigma, UK.), penicillin (1,000 units/ml) and streptomycin (0.1 mg/ml) (Sigma, UK) and 2 mM L-Glutamate (Gibco, UK). Cells were grown to confluency in T75cm² flasks and routinely passaged at a 1:3 dilution every 3-4 days.

Cell Transfection

For expression of STAT92E-GFP or Dome-FLAG, cells were seeded a day prior to transfection. They were transfected at a ratio of 2 µg DNA/$1x10^6$ cells in a 6 well plate, using Effectene Reagent (Qiagen Ltd, UK) and used 2 days later for experiments.

Upd2-GFP production

Upd2-GFP conditioned media was produced essentially as described (Wright et al., 2011) with the following modifications: S2R+ cells were seeded at $1x10^6$ cells per well of a 6-well plate 1 day prior to transfection. pAct-Upd2-GFP (2µg per well) was transfected using Effectene Transfection Reagent (Qiagen Ltd, UK) following the manufacturer's instructions. After 2 days, 3 wells of transfected cells were transferred to a T75 cm² flask and incubated for a further 4 days. Cells were centrifuged at 1000 x *g* for 3mins, and media was filtered, aliquoted and snap-frozen in liquid N_2 and stored at -80°C. The concentration of Upd2-GFP was determined using an ELISA for GFP (see below). Mock conditioned media (referred to as mock treatment) was produced by transfecting cells with 2 µg pAc5.1 and processed as above.

dsRNA knockdown

dsRNAs were obtained from the Sheffield RNAi Screening Facility whose dsRNA database is based on the Heidelberg 2 library (Boutros lab), generated with Next-RNAi (Horn et al., 2010). It is the redesigned, non-off target effect library, HD2.0 generated using the software next-RNAi (developed by Thomas Horn). Low complexity regions and sequence motifs that induce off-target effects have been excluded. dsRNA probe sizes vary from 81 to 800bp covering ~14000 protein encoding genes and ~1000 non-coding genes (~98.8% coverage). The dsRNA design covers every isoform of each gene and has been optimised for specificity and avoidance of low complexity regions. The following dsRNA amplicons were used; Alpha-adaptin (BKN20148); CHC (BKN20463); Dome (BKN25660); Hrs (BKN27923); TSG101 (BKN28961). Negative control dsRNA was a mixture of 3 amplicons

566 targeting *C. elegans* mRNA (BKN70003, BKN70004, BKN70005). Amplification of

567 dsRNA was carried out using MEGAscript® RNAi Kit (Life Technologies #AM1626),

568 and purified via ethanol precipitation with sodium acetate, followed by resuspension

569 in sterile water.

570 Cells were seeded one day prior to knockdown, and resuspended in serum free

571 media on the day of knockdown. The desired number of cells was added to the wells

572 already containing dsRNA and incubated for 1hr at 25°C (15 µg of dsRNA plus 1×10^6

573 cells per well in a 6-well plate). After incubation, an equal volume of fresh media

574 containing 20% FBS was added. Cells were incubated at 25°C for a total of 5 days

575 before subsequent experiments. Transfection with STAT92E-GFP was performed on

576 day 3 of dsRNA treatment.

577

578 **Generation of CRISPr S2R+ cell lines**

579 sgRNA were designed to target the N-terminal coding region of STAT92E and

580 showed <1% chance of off-target activity (crispr.mit.edu). Sequences were also

581 verified using NCBI blast to eliminate potential off-targets. The NGG sequence was

582 then removed, and a G was added to the 5' end of the sgRNA sequence to allow

583 transcription from the U6 promoter in pAc-sgRNA-Cas9 vector. sgRNA oligos (Table

584 1) were cloned into the pAc-sgRNA-Cas9 expression vector according to the

585 published protocol (Bassett et al., 2014). S2R+ cells were plated at 5×10^5 cells per well

586 in a 12-well plate and transfected with 1 µg pAc-sgRNA-Cas9 construct using

587 Effectene (Qiagen Ltd, UK). After 3 days, puromycin (5 µg ml^{-1}) selection was

588 performed for 7 days before subsequent analysis (Bassett et al., 2014).

Table 1: SgRNA oligos
sgRNA1.1: TTCGACAACACGCCCATGGTTACC
sgRNA1.1: AACGGTAACCATGGGCGTGTTGTC
sgRNA2.1 TTCGACCATGTACCCGGTAACCAT
sgRNA2.2 AACATGGTTACCGGGTACATGGTC

589 To detect Cas9 induced mutations within the genomic DNA of S2R+ CRISPR cell

590 lines, a T7 endonuclease assay was carried out to identify mismatched, heteroduplex,

591 DNA. PCR products were first produced by amplifying a ~1 kb region around the

592 Cas9 cut site with a 50 µl PCR reaction according to the following method (Guschin

593 et al., 2010). Following verification of size on agarose gels, PCR products were

594 denatured and annealed to form heteroduplexes in the following reaction: 5-10 µl

595 PCR products, 2 µl NEBuffer 2 made up to 19 µl with nuclease free water. The

596 reaction was heated at in a 95°C heat block for 10mins and allowed to cool to room

597 temperature. 1 µl of T7 endonuclease was then added to reactions and incubated at

598 37°C for 15 mins. The reaction was stopped by addition of 1.5 µl 0.25 M EDTA

599 before running on an agarose gel.

600

601 **ELISA assay for GFP**

602 The anti-GFP ELISA was performed essentially as described (Wright et al., 2011).

603 Briefly, 96-well high-binding EIA plate (Costar) was coated with 0.0625 µg ml^{-1} goat

604 anti-GFP antibody (Abnova #PAB10341) in 100mM Sodium Bicarbonate overnight at

605 4°C. The plate was washed 3x with wash buffer (0.2% (w/v) BSA, 0.5% Triton-X 100

606 in PBS) and then blocked in the same buffer for 1 h at RT. A serial dilution of

607 recombinant GFP (Cellbiolabs, STA-201), starting at 5 ng ml^{-1}, was plated for

608 reference. Samples were incubated for 3 h at 37°C. After washing, the plate was

609 incubated with rabbit anti-GFP (Abcam, Ab290) at 1:20,000 for 2h at RT. After further

610 washes, the plate was incubated with a secondary HRP-linked anti-rabbit antibody

611 (Santa Cruz, sc-2004) at 1:5000 for 1h at RT. Following washing, 200 µl per well of

612 freshly prepared HRP developing solution (0.012% H_2O_2, 0.4 mg ml^{-1} o-

613 phenylenediamine in HRP assay buffer: 51 mM Na_2HPO_4, 27 mM citric acid, pH 5.0,

614 (filtered)) was added to the plate and colour change was observed. To stop the

615 reaction 50 µl of 2 M H_2SO_4 was added per well and the absorbance read at 492 nm

616 on a BMG Labtech plate reader.

617

618 **Endocytosis assays using anti-GFP ELISA**

619 Cells were seeded in a 24 well plate (2x10^5 cells per well) a day prior to experiment.

620 Media was replaced with conditioned media containing established concentrations of

621 Upd2-GFP and incubated at 25°C for various times. Endocytosis was stopped by

622 placing cells on ice and washing twice with ice-cold PBS. Cell-surface ligand was

623 removed by 2x acid washing with 0.2M glycine, 0.15M NaCl pH 2.5 for 2mins. Cells

624 were then washed again in PBS before lysis in ELISA lysis buffer (PBS containing 1

625 mM MgCL$_2$, 0.1% (w/v) BSA, 0.5% Triton-X 100 supplemented with cOmplete™, Mini,

626 EDTA-free Protease Inhibitor Cocktail (Roche #11836170001)).

627

628 **Endocytosis assays using cell surface biotinylation**

629 All reactions were carried out on ice unless specified. Growth media was aspirated

630 from cells which were washed 2x with ice-cold PBS. Cells were incubated for 1 hr on

631 ice with freshly prepared EZ-linkTM Sulfo-NHS-SS-Biotin (Thermo Scientific™) (0.25

632 mg ml^{-1}) before biotin was quenched by washing twice with PBS containing 100 mM

633   glycine. Internalisation was allowed to proceed for various times by adding pre-

634   warmed Upd2-GFP and incubating at 25°C. Cells were returned to ice and washed

635   2x with PBS. Cell surface biotin was cleaved by washing cells 3x for 20 mins with

636   MESNa (100 mM 2-mercaptoethanesulfonate, added fresh for each incubation to

637   50mM Tris-HCL pH8.6, 100 mM NaCl, 1 mM EDTA, 0.2% (w/v) BSA). Cells were

638   then washed 3x in PBS. Reduced disulphide bonds were alkylated for 10mins with

639   500 mM Iodoacetamide in PBS, before a final 2x PBS wash. Cells were then lysed

640   for 30 mins and lysates were centrifuged at 13,000 rpm for 10 mins. Streptavidin-

641   agarose (15µl) was washed 3x with lysis buffer and incubated with cell lysate (10-

642   30µg) overnight at 4°C with rotation. Beads were then washed 3x with lysis buffer

643   and boiled for 5mins at 95°C in 20 µl Laemmli SDS-PAGE buffer before SDS-PAGE

644   and Western blotting.

645

646   Lysis buffer: 20 mM Tris pH7.5, 150 mM NaCl, 1 mM EDTA, 1 mM EGTA, 1% Triton

647   X-100, 1 mM β-Glycerophosphate, 25 mM Na-Pyrophosphate, 1 mM Na_3VO_4,

648   1 µg ml^{-1} microcystin, 25mM N-ethylmaleimide supplemented with cOmplete™,

649   Mini, EDTA-free Protease Inhibitor Cocktail (Roche #11836170001).

650

651   ***10xSTAT-Luciferase* detection**

652   Cells were seeded in a 12-well plate at 5×10^5 cells per well a day prior to transfection.

653   Cells were transfected with 0.5 µg *10xSTAT-luciferase* and 0.5 µg pAct-Renilla

654   (internal control for transfection) for 1 day and then transferred to a 96-well plate at

655   5×10^4 cells per well. Cells were treated with conditioned media containing Upd2-GFP

656   for 18hrs. Luciferase activity was measured using the Dual-Glo Luciferase Assay

657   System (Promega), following manufacturer's instructions, using a 1:5 dilution of

658   DualGlo-luciferase in distilled water. The Dual-Glo Stop and Go Luciferase Assay

659   reagent (1:5 dilution) was added to the plate at an equal volume to the culture media

660   in the wells, and incubated for at least 10mins. The Luciferase firefly signal was

661   measured using a Thermo Scientific™ Varioskan Flash Luminometer. An equal

662   volume of Dual-Glo Stop & Glo Reagent was then added and incubated for at least a

663   further 10 mins to allow measurement of the Renilla firefly (RL) signal. Luciferase

664   activity is calculated as Firefly luciferase value normalized to the internal transfection

665   control (RL).

666

667   **Calf intestinal alkaline phosphatase (CIP) treatment**

668   STAT92E was immunoprecipitated from cells lysed in lysis buffer (PBS containing 1

669   mM $MgCl_2$, 0.1% (w/v) BSA, 0.5% Triton-X 100 supplemented with cOmplete™, Mini,

670 EDTA-free Protease Inhibitor Cocktail (Roche)). CIP (#M0290S NEB) 1 unit per 1μg

671 protein was incubated for 1 hr at 37°C. Reaction was stopped by addition of sample

672 buffer and boiling at 95°C for 5 mins.

673

674 **Quantitative PCR**

675 RNA extraction was carried out using TRI reagent (Sigma #T9424) and reverse

676 transcribed using the High Capacity RNA-tocDNA™ Kit (Applied Biosystems

677 #4387406). cDNA was diluted 1:10 and relative mRNA levels of *socs36E, Dome*,

678 *lama, AP2, Hrs* and *TSG101* were quantified using qPCR. This was performed using

679 SYBR Green JumpStart™ Taq ReadyMix™ (Sigma #S4438) and primers, listed in

680 Table 2, on the BioRad CFX96 Real time system, C100 Touch™ thermal cycler or the

681 Applied Biosystem QuantStudio 12K Flex. A standard curve of diluted template was

682 used to interpolate the quantity of target gene in the test samples. Results for each

683 target were normalised to levels of the reference gene, ribosomal protein L32 (Rpl32)

684 mRNA, within each well.

Table 2	Primers for qPCR		
Gene	CG number	Forward primer	Reverse primer
Rpl32	CG7939	GACGCTTCAAGGGACAGTATCTG	AAACGCGGTTCTGCATGAG
domeless	CG14226	ACTTTCGGTACTCCATCAGC	TGGACTCCACCTTGATGAG
tsg101	CG9712	GAGGAGACACAAATAACAAAGTACC	TGAGTGTCCATCAACCAAATAC
clathrin heavy chain CHC	CG9012	GTAGTAAAGATGACGCAACCAC	GTTCATGTCAATGATGACCACT
α-adaptin	CG4260	ACCAGCGAAAATTAACAAGC	GAGACGACTTCACACCCTTC
socs36A	CG15154	AGTGCTTTACTGCTGCGACT	TCGTCGAGTATTGCGAAGT
lama	CG10645	TGATATTGCTGCTTTCCTGGAC	TGGTTTGGCGATGGTTTTAT

685

686 **Site-directed mutagenesis**

687   Site-directed mutagenesis was carried out using the QuikChange Site-Directed

688   Mutagenesis Kit (Agilent Technologies) according to manufacturer's instructions.

689   Sequencing of plasmid DNA was carried out at the University of Sheffield's Core

690   Genomic Facility and results analysed using ApE.

691

692   **Mass spectrometry methods**

693   A detailed description of mass spectrometry methods (sample preparation, mass

694   spectrometry analysis and data processing) together with mass spectrometry data

695   and annotated relevant spectra (phosphorylated Y704, T47, S227, and T702) has

696   been deposited to the ProteomeXchange Consortium via the PRIDE partner

697   repository (Deutsch et al., 2020). The identifier number of the dataset is PXD020719.

698

699   **Immunofluorescence detection of nuclear and cytoplasmic STAT92E-GFP**

700   A DeltaVision/GE Healthcare OMX optical microscope (version 4) with oil-immersion

701   objective (60x NA 1.42, PlanApochromat Olympus) was used for widefield and SIM

702   immunofluorescence image acquisition. Deconvolution and image registration (for

703   alignment of SIM images) was carried out using the DeltaVision OMX softWoRx 6.0

704   software. Analysis of microscopy images was carried out using ImageJ. Four regions

705   of interest (ROI) of equal size were drawn within each transfected cell: two within the

706   nucleus and two within the cytoplasm. Intensity measures were averaged for the

707   nucleus and divided by the average intensity for the cytoplasm.

708

709

720 **Abbreviations:**

721 JAK/STAT: Janus Kinase/Signal transducer and activator of transcription

722 CME: clathrin-mediated endocytosis

723 CIE: clathrin independent endocytosis

724 ESCRT: Endosomal sorting complexes required for transport

725 Dome: Domeless

726 EGFR: epidermal growth factor receptor

727 RL: Renilla Luciferase

728 FL : 10xSTAT-Luciferase

729 CIP: Calf intestinal phosphatase

730

731

732

Figure Legends

734 *Figure 1: Uptake of Upd2-GFP into S2R+ cells is Dome-, clathrin-, and AP2*

735 *dependent*

736 (A) S2R+ cells were treated for 5 days with control, clathrin (CHC), AP2, or Dome

737 dsRNA. Cells were incubated with 20 nM Upd2-GFP for indicated time points at

738 25°C. Following acid washes, cell lysates were analysed with an anti-GFP ELISA.

739 Internalised Upd2-GFP is expressed as percentage of the total amount internalised

740 at 30 minutes. Data represent mean +/- s.d. of two independent experiments. Data

741 were fitted using the non-linear least squares fit in Prism.

742 (B) Schematic of *Drosophila* Dome and the vertebrate gp130/IL6-R complex.

743 (C) A di-Leu cassette in the cytoplasmic tail of gp130 and Dome, and mutants

744 generated to investigate internalisation motifs. Note Dome^{AAASKAAL} is referred to as

745 Dome^{allA} in the text.

746 (D) Quantitation of internalisation of Dome-FLAG wild-type and mutants: Percentage

747 of cell-surface receptor that is internalised after 15 mins at 25°C. Background of

748 biotinylated cell surface Dome-FLAG after 0 mins endocytosis and MESNa treatment

749 was subtracted and internalised Dome-FLAG was then calculated as a percentage of

750 total cell surface Dome-FLAG prior to MESNa treatment. Graphs represent mean +/-

751 s.e.m. for at least 3 independent experiments (Dome$^{E980A/LL985AA}$ = 3 repeats, all other

752 mutants ≥ 4 repeats). *: $p<0.5$; **: $p<0.01$; ***: $p< 0.001$

753 (E) Sample immunoblot of lysates from cells transfected with Dome^{WT}-FLAG,

754 Dome^{allA}-FLAG, Dome^{LL985AA}-FLAG, Dome$^{E980G/LL985AA}$-FLAG, Dome$^{S979A/LL985AA}$-FLAG,

755 or Dome$^{S981A/LL985AA}$-FLAG, for 48 hrs prior to cell surface biotinylation and incubation

756 at 25°C for times indicated +/- Upd2-GFP and +/-MESNa. Western blots were probed

757 with antibodies as indicated.

758

759 *Figure 2: Endocytosis regulates Dome target gene expression.*

760 (A)   Expression of *10xSTAT-Luciferase* reporter is Upd2-GFP dependent. S2R+

761 cells were transfected with an actin driven Renilla Luciferase (RL) and *10xSTAT-*

762 *Luciferase* (FL) reporter construct for 6hrs and then treated with varying

763 concentrations of Upd2-GFP for 30mins, followed by incubation for 18hrs in fresh

764 media, before bioluminescence was measured. Graph represents mean +/- s.d. of 2

765 experiments, each performed in triplicate.

766 (B) Mutation of Dome internalisation motifs inhibits Upd2-GFP-induced *10xSTAT-*

767 *Luciferase* reporter activation. S2R+ cells were transfected with pAc- Ren (RL),

768 *10xSTAT-luciferase* (FL) reporter and pAc5.1 (-) and Dome^{WT}-FLAG, Dome^{allA}-FLAG,

769 Dome$^{Y966A/Q969A}$-FLAG or Dome^{P925I}-FLAG. Cells were stimulated with 0.75 nM Upd2-

770   GFP for 30 mins, then incubated in fresh media for 18 hrs. Luciferase activity (FL/RL)

771   is presented as a fold change compared to mock treated cells transfected with pAc5.1 (-).

772   Graph represents mean of triplicates +/- s.e.m. for 4 independent experiments.

773   Parametric, unpaired student's t-test was performed, **: $p \leq 0.01$, ***: $p \leq 0.001$, ns: not

774   significant.

775   (C) S2R+ cells were transfected with RL and FL for 6hrs prior to treatment with

776   dsRNA targeting Dome, AP2, Hrs or TSG101 or control (non-targeting), and

777   incubated for five days. Cells were treated with Upd2-GFP for 18hrs and then

778   bioluminescence was measured. Luciferase activity (FL/RL) is normalised to control,

779   mock treated, cells. Graph represents mean of triplicates +/- s.e.m. for 4 experiments.

780   Parametric, unpaired student's t-test carried out to compare Upd2-GFP stimulated

781   samples only, with *: $p \leq 0.05$, ****: $p \leq 0.0001$.

782   (D) S2R+ cells were treated with dsRNA against AP2, Hrs and TSG101 as well as

783   non-targeting (control) dsRNA for 5 days. Cells were incubated with 3 nM Upd2-GFP

784   for 2.5 hrs prior to RNA extraction. *socs36* mRNA levels were normalised to that of

785   reference gene Rpl32, and presented as fold change compared to mock-treated

786   control samples. Results are expressed as means of triplicates +/- s.e.m. for 3

787   independent experiments. Parametric, unpaired student's t-test was carried out to

788   compare Upd2-GFP stimulated samples only. **: $p \leq 0.01$

789

790   ***Figure 3: Tyr704 phosphorylation of STAT92E is independent of endocytic***

791   ***regulation***

792   (A) Western blot showing that Upd2-GFP causes a concentration dependent

793   bandshift, indicative of phosphorylation, of STAT92E. The positions of the non-

794   phosphorylated and phosphorylated forms are indicated on the blot.

795   (B) Graph represents quantitation of phosphorylated STAT92E as a function of

796   Upd2-GFP concentration. Phosphorylated STAT92E is expressed a % of total

797   STAT92E.

798   (C) S2R+ cells were treated with 3 nM Upd2-GFP for 10mins and lysates incubated

799   with anti-STAT92E antibodies. Immunoprecipitated protein was then treated with calf

800   intestinal phosphatase (CIP), and analysed by SDS-PAGE and immunoblotting with

801   anti-STAT92E antibodies. p-STAT92E and STAT92E are indicated by arrows.

802   (D) Quantitation of p-STAT92E/STAT92E ratio +/- phosphatase treatment

803   (E) Representative immunoblot of control vs AP2 knockdown S2R+ cells treated with

804   3 nM Upd2-GFP at 25°C for the indicated times. Cells were treated with targeting

805   dsRNA cells and incubated for 5 days at 25°C. Total protein extract was analysed by

806   SDS-PAGE and immunoblotted with anti-STAT92E antibodies.

807   (F) Quantification of STAT92E phosphorylation after AP2 knockdown.

808   Phosphorylated STAT92E is expressed as % total STAT92E. Results are expressed

809   as mean +/- s.e.m. from 4 independent experiments. Using student's t-test there are

810   no statistically significant differences between control and AP2 knockdown samples.

811   (G) Upd2-dependent phosphorylation of Tyr704 is unchanged following dsRNA

812   mediated knockdown of AP2. S2R+ cells treated with control and AP2 dsRNA were

813   transfected with STAT92E-GFP and treated with 3 nM Upd2-GFP for 75 min. Cells

814   were lysed and incubated with GFP-trap beads prior to preparation for mass

815   spectrometry analysis. Histograms present the ratios Mod/Base of the Y704

816   phosphorylation site from STAT92E-GFP calculated by MaxQuant software in all

817   conditions. Data shown for n=1.

818

819   ***Figure 4: Upd2-dependent nuclear translocation of STAT92E requires Tyr704***

820   ***phosphorylation but is independent of endocytosis***

821   (A) Representative images of cells treated with control dsRNA or dsRNA targeting

822   Dome, AP2 or Hrs for 5 days and transfected with STAT92E^{WT}-GFP (day 3) and

823   treated with 3 nM Upd2-GFP for 0 or 30 mins.

824   (B) Time-course of nuclear accumulation of STAT92E-GFP following treatment with

825   Upd2-GFP. Nuclear signal was divided by cytoplasmic signal, and expressed as a

826   percentage of nuclear STAT92E-GFP after 30mins. Data are presented as mean +/-

827   s.d. for at least two independent experiments where >15 cells were examined per

828   experiment.

829   (C) Quantitation of nuclear versus cytoplasmic STAT92E^{wt}-GFP and STAT92E^{Y704F}-

830   GFP following treatment of cells with Upd2-GFP for the times indicated. Nuclear

831   signal was divided by cytoplasmic signal, and normalised to 0mins in control cells.

832   Data are presented as mean +/- s.e.m. where at least 80 cells were imaged from 3

833   independent experiments.

834   (D) Quantitation of nuclear STAT92E-GFP versus cytoplasmic STAT92E-GFP

835   following treatment of cells with control dsRNA or dsRNA targeting Dome, AP2 or

836   Hrs. Nuclear signal was divided by cytoplasmic signal, and normalised to 0 mins

837   control cells. Data are presented as mean +/- s.e.m. for 3 independent experiments

838   where at least 20 cells were imaged per condition per experiment, with parametric,

839   unpaired student's t-test being performed. ****: p≤0.0001; ns is non significant.

840

841   ***Figure 5: Phosphorylation of Thr702 on STAT92E is essential for its function***

842   (A) Schematic of STAT92E indicating domains, Tyr704 and novel phosphorylation

843   sites that were identified by mass spectrometry.

844   (B) Control (WT) or cells lines lacking STAT92E (crSTAT) cell lines were transfected

845   with pAc- Ren (RL), *10xSTATluciferase* (FL) reporter and pAc5.1(-) for 24 hrs. Cells

846   were stimulated with 3 nM Upd2-GFP for 30 mins, and then incubated in fresh media

847   for 18 hrs. Luciferase activity (FL/RL) is expressed as a fold change compared to mock

848   treated cells transfected with pAc5.1 (-). Graph represents mean +/- s.e.m. of triplicates

849   from 3 independent experiments. Parametric, unpaired student's t-test was

850   performed with ****: $p \leq 0.0001$.

851   (C) STAT92E mutants which cannot be phosphorylated, STAT92E^{T702V} and

852   STAT92E^{Y704F}, inhibit Upd2-GFP-dependent signalling. crSTAT cells were

853   transfected with pAc-Ren, *10xSTAT-Luciferase* and pAc5.1 (-), and/or STAT92E-

854   GFP mutants as indicated. Cells were mock-treated or stimulated with 0.75 nM

855   Upd2-GFP for 30 mins, and then incubated in fresh media for 18 hrs. Data are mean

856   +/- s.e.m. from 3 independent experiments, each performed in triplicate and

857   normalised to cells transfected with pAc5.1 (-). Parametric, unpaired student's t-test

858   was performed with **: $p \leq 0.01$, ****: $p \leq 0.0001$.

859   (D) Phosphomimetic forms of STAT92E rescue inhibitory effects of T702V on Upd2-

860   GFP-dependent signalling. crSTAT cells were transfected with pAc-Ren, *10xSTAT-*

861   *Luciferase* and pAc5.1 (-) and/or STAT92E-GFP mutants as indicated. Cells were

862   mock-treated or stimulated with 0.75 nM Upd2-GFP for 30 mins, then incubated in

863   fresh media for 18 hrs. Luciferase activity (FL/RL) is expressed as a fold change

864   compared to mock treated cells transfected with pAc5.1 (-). Data is expressed as mean

865   +/- s.e.m. from 3 independent experiments and normalised to mock-treated cells

866   transfected with pAc5.1. Parametric, unpaired student's t-test was performed, with *:

867    $p \leq 0.05$, **: $p \leq 0.01$, ***: $p \leq 0.001$, ns: non significant.

868

869   ***Figure 6: Phosphorylation of Thr702 is essential for Tyr704 phosphorylation***

870   (A) T702V mutation prevents STAT92E-GFP nuclear translocation in response to

871   ligand. Representative images of crSTAT cells transfected with either STAT92E^{WT}-

872   GFP or STAT92E^{T702V}-GFP, and treated with 3 nM Upd2-GFP for 0, 15 or 30 mins.

873   (B) Nuclear signal was divided by cytoplasmic signal, and normalised to 0 mins

874   control cells. Data is presented as mean +/-s.e.m. for 3 independent experiments,

875   where at least 30 cells were imaged per condition per experiment. Parametric,

876   unpaired student's t-test being performed. ****: $p \leq 0.0001$, ns: non significant

877   (C) Mutation of Thr702 reduces phosphorylation on Tyr704. S2R+ cells were

878   transfected with STAT92E^{WT}-GFP or STAT92E^{T702V}-GFP for 2 days prior to treatment

879   with 3nM Upd2-GFP for 75mins. Cells were lysed and incubated with GFP-trap

880   beads prior to preparation for mass spectrometry analysis. Histograms present the

881 ratios Mod/Base of Y704 phosphorylation site from STAT92E^{WT}-GFP and

882 STAT92E^{T702V}-GFP calculated by MaxQuant software. Data shown for n=1.

883 (D) Compartmentalised signalling regulates expression of JAK/STAT targets.

884 Cartoon depicting how movement of the Upd2/Dome complex along the endocytic

885 pathway regulates differential gene expression. At the cell surface activated Dome

886 can result in transcription of a subset of target genes (e.g. *lama*, shown in green).

887 Following uncoating of clathrin and AP2 from clathrin coated vesicles, other genes

888 can be activated (e.g. *Luciferase*, shown in orange). Hrs selects ubiquitinated cargo

889 for incorporation into intraluminal vesicles but activated Dome can still signal to

890 activate other genes (e.g. *socs36E*, shown in purple) before TSG101 results in its

891 incorporation into inward invaginations of the endosomal membrane to form intra

892 luminal vesicles which results in termination of signalling.

893 (E) Thr702 conservation and location within STAT1 crystal structure. (i) Alignment of

894 sequences surrounding the conserved Tyr in STAT92E-C (C isoform), STAT92E-F

895 (long isoform), human STAT1, STAT5a and STAT5b. The conserved Tyr is

896 highlighted in orange, and a conserved Lys highlighted in green. The Thr residue is

897 in a yellow box. ii) Crystal structure of STAT1 (PDB:1bf5). iii) Location of the Thr and

898 Tyr residues within the STAT1 crystal structure.

899

900

Supplementary Legends

902 **Figure S1:**

903 (A) CME is the route of GFP-Upd2 uptake at low ligand concentrations.

904 S2R+ cells were treated for 5 days with control, clathrin (CHC) or Dome dsRNA.

905 Cells were incubated with 3 nM Upd2-GFP for indicated time points at 25°C.

906 Following acid washes, cell lysates were analysed with an anti-GFP ELISA.

907 Internalised Upd2-GFP is expressed as percentage of the total amount internalised

908 at 30 minutes. Graph is a representative experiment where each point is mean of

909 triplicates +/- s.d.

910 (B) mRNA levels of dsRNA targets following knockdown. S2R+ cells were treated

911 with dsRNA 5 days prior to TRIzol RNA extraction. mRNA levels were analysed

912 using qPCR, with levels of target mRNA normalised to rpl32 mRNA. Ratios are

913 plotted as fold change compared to control dsRNA for each target mRNA. Graph

914 represents the mean of triplicates +/- s.d. for at least 2 independent experiments

915 (Dome = 2 repeats), or mean +/- s.e.m. for at least three independent experiments

916 (AP2, Hrs and TSG101). Parametric, unpaired student's t-test was performed to

917 compare control knockdown with targeted dsRNA knockdown, with ***p≤0.001,

918 ****p≤0.0001.

919 (C) Lysates from S2R+ cells transfected with FLAG-tagged Dome wild-type and

920 mutants were prepared and subjected to SDS-PAGE and Western blotting with

921 antibodies to FLAG and β-actin. The ratio of transfected Dome-FLAG construct is

922 expressed as a function of the amount of β-actin. Graph is the mean ± s.d. of at least 2

923 independent experiments. Using student's t-test, there was no statistical difference

924 between wild-type and mutant constructs.

925 (D) Percentage of biotinylated Dome-FLAG at cell surface compared to total levels of

926 transfected Dome-FLAG in cells expressing wild-type or mutant Dome-FLAG

927 constructs. Using student's t-test, there was no statistical difference between wild-type

928 and mutant constructs.

929 (E) Dome is internalised efficiently in the absence of ligand. Sample immunoblot of

930 cells transfected with Dome[WT]-FLAG for 48hrs prior to cell surface biotinylation and

931 endocytosis for 15 minutes +/- Upd2-GFP, followed by treatment +/- MESNa.

932 Western blots were probed with antibodies as indicated.

933 (F) Sample immunoblot of lysates from cells transfected with Dome[WT]-FLAG or

934 Dome[E980A]-FLAG for 48 hrs prior to cell surface biotinylation and incubation at 25°C

935 for times indicated +/- Upd2-GFP followed by treatment +/- MESNa. Western blots

936 were probed with antibodies as indicated.

937   (G) Quantitation of internalisation of Dome^{WT}-FLAG and Dome^{E980A}-FLAG.

938   Percentage of cell-surface receptor that is internalised after 15 mins at 25°C.

939   Background of biotinylated cell surface Dome-FLAG after 0 mins endocytosis and

940   MESNa treatment was subtracted and internalised Dome-FLAG was then calculated

941   as a percentage of total cell surface Dome-FLAG prior to MESNa treatment. Graphs

942   represent mean +/- s.d. for 2 independent experiments and no significant differences

943   were observed.

944

945   **Figure S2**:

946   (A) Sample immunoblot of relative transfection efficiencies of Dome^{WT}-FLAG,

947   Dome^{allA}-FLAG, Dome$^{Y966A/Q969A}$-FLAG and Dome ^{P925I}-FLAG. Blots were probed with

948   antibodies as indicated.

949   (B) *lama* expression is independent of endocytosis. S2R+ cells were treated with

950   dsRNA against AP2, Hrs and TSG101 as well as non-targeting (control) dsRNA for 5

951   days. Cells were incubated with 3 nM Upd2-GFP for 2.5 hrs prior to RNA extraction.

952   *lama* mRNA levels were normalised to that of reference gene Rpl32, and presented

953   as fold change compared to mock-treated control samples. Results are expressed as

954   means of triplicates +/- s.e.m. for 3 independent experiments.

955

956   **Figure S3**: STAT92E phosphorylation is not regulated by endocytosis.

957   Representative immunoblot of control vs AP2, Hrs and TSG101 knockdown S2R+

958   cells treated with 3 nM Upd2-GFP at 25°C for the indicated times. Cells were treated

959   with targeting dsRNA and incubated for 5 days at 25°C. Total protein extract was

960   analysed by SDS-PAGE and immunoblotted with anti-STAT92E antibodies.

961

962   **Figure S4:** Generation and characterization of STAT92E negative S2R+ cells.

963   (A) Immunoblot and quantification demonstrating levels of STAT92E protein in cells

964   transfected with pAc-sgRNA-Cas9 targeting STAT92E for 3 days, and then either

965   with or without puromycin selection as indicated. Blots were probed with antibodies

966   as indicated.

967   (B) T7-endonuclease assay demonstrates Cas9 induced mutation in the STAT92E

968   gene. Genomic DNA was extracted from WT and crSTAT2 cell lines, and a 989bp

969   region around the sgRNA target site was amplified by PCR. Addition of T7

970   endonuclease to the PCR product causes multiple bands for crSTAT2 cell line but

971   not WT cells.

972   (C) Mutation of Lys187 increases STAT92E signalling. crSTAT cells were transfected

973   with pAc-Ren, *10xSTAT-Luciferase* and pAc5.1 (-), STAT92E^{WT}-GFP or

974   STAT92E^{K187R}-GFP. Cells were stimulated with 0.75 nM Upd2-GFP for 30 mins, then

975   incubated in fresh media for 18 hrs followed by measurement of bioluminescence.

976   Data is mean +/- s.e.m. from 3 independent experiments and normalised to cells

977   transfected with pAc5.1 (-) and treated with 0 nM Upd2-GFP. *: $p < 0.05$; **: $p < 0.01$.

978

979

980   **References**

981   **Baeg, G. H., Zhou, R. and Perrimon, N.** (2005). Genome-wide RNAi
982   analysis of JAK/STAT signaling components in Drosophila. *Genes Dev* **19**, 1861-70.
983   **Bassett, A. R., Tibbit, C., Ponting, C. P. and Liu, J. L.** (2014). Mutagenesis
984   and homologous recombination in Drosophila cell lines using CRISPR/Cas9. *Biol*
985   *Open* **3**, 42-9.
986   **Begitt, A., Meyer, T., van Rossum, M. and Vinkemeier, U.** (2000).
987   Nucleocytoplasmic translocation of Stat1 is regulated by a leucine-rich export signal
988   in the coiled-coil domain. *Proc Natl Acad Sci U S A* **97**, 10418-23.
989   **Brown, S., Hu, N. and Hombria, J. C.** (2001). Identification of the first
990   invertebrate interleukin JAK/STAT receptor, the Drosophila gene domeless. *Curr Biol*
991   **11**, 1700-5.
992   **Brown, S. and Zeidler, M. P.** (2008). Unphosphorylated STATs go nuclear.
993   *Curr Opin Genet Dev* **18**, 455-60.
994   **Carroll, B. and Dunlop, E. A.** (2017). The lysosome: a crucial hub for AMPK
995   and mTORC1 signalling. *Biochem J* **474**, 1453-1466.
996   **Cendrowski, J., Maminska, A. and Miaczynska, M.** (2016). Endocytic
997   regulation of cytokine receptor signaling. *Cytokine Growth Factor Rev* **32**, 63-73.
998   **Chanut-Delalande, H., Jung, A. C., Baer, M. M., Lin, L., Payre, F. and**
999   **Affolter, M.** (2010). The Hrs/Stam complex acts as a positive and negative regulator
1000   of RTK signaling during Drosophila development. *PLoS One* **5**, e10245.
1001   **Chen, X., Vinkemeier, U., Zhao, Y., Jeruzalmi, D., Darnell, J. E., Jr. and**
1002   **Kuriyan, J.** (1998). Crystal structure of a tyrosine phosphorylated STAT-1 dimer
1003   bound to DNA. *Cell* **93**, 827-39.
1004   **Cherbas, L., Willingham, A., Zhang, D., Yang, L., Zou, Y., Eads, B. D.,**
1005   **Carlson, J. W., Landolin, J. M., Kapranov, P., Dumais, J. et al.** (2011). The
1006   transcriptional diversity of 25 Drosophila cell lines. *Genome Res* **21**, 301-14.
1007   **Chmiest, D., Sharma, N., Zanin, N., Viaris de Lesegno, C., Shafaq-Zadah,**
1008   **M., Sibut, V., Dingli, F., Hupe, P., Wilmes, S., Piehler, J. et al.** (2016).
1009   Spatiotemporal control of interferon-induced JAK/STAT signalling and gene
1010   transcription by the retromer complex. *Nat Commun* **7**, 13476.
1011   **Chung, J., Uchida, E., Grammer, T. C. and Blenis, J.** (1997). STAT3 serine
1012   phosphorylation by ERK-dependent and -independent pathways negatively
1013   modulates its tyrosine phosphorylation. *Mol Cell Biol* **17**, 6508-16.
1014   **Costa-Pereira, A. P., Bonito, N. A. and Seckl, M. J.** (2011). Dysregulation
1015   of janus kinases and signal transducers and activators of transcription in cancer. *Am*
1016   *J Cancer Res* **1**, 806-16.
1017   **Deutsch, E. W., Bandeira, N., Sharma, V., Perez-Riverol, Y., Carver, J. J.,**
1018   **Kundu, D. J., Garcia-Seisdedos, D., Jarnuczak, A. F., Hewapathirana, S.,**
1019   **Pullman, B. S. et al.** (2020). The ProteomeXchange consortium in 2020: enabling
1020   'big data' approaches in proteomics. *Nucleic Acids Res* **48**, D1145-D1152.
1021   **Devergne, O., Ghiglione, C. and Noselli, S.** (2007). The endocytic control of
1022   JAK/STAT signalling in Drosophila. *J Cell Sci* **120**, 3457-64.
1023   **Di Guglielmo, G. M., Le Roy, C., Goodfellow, A. F. and Wrana, J. L.**
1024   (2003). Distinct endocytic pathways regulate TGF-beta receptor signalling and
1025   turnover. *Nat Cell Biol* **5**, 410-21.
1026   **Dittrich, E., Haft, C. R., Muys, L., Heinrich, P. C. and Graeve, L.** (1996). A
1027   di-leucine motif and an upstream serine in the interleukin-6 (IL-6) signal transducer
1028   gp130 mediate ligand-induced endocytosis and down-regulation of the IL-6 receptor.
1029   *J Biol Chem* **271**, 5487-94.
1030   **Doray, B., Lee, I., Knisely, J., Bu, G. and Kornfeld, S.** (2007). The
1031   gamma/sigma1 and alpha/sigma2 hemicomplexes of clathrin adaptors AP-1 and AP-
1032   2 harbor the dileucine recognition site. *Mol Biol Cell* **18**, 1887-96.

1033   **Ekas, L. A., Cardozo, T. J., Flaherty, M. S., McMillan, E. A., Gonsalves, F.**
1034 **C. and Bach, E. A.** (2010). Characterization of a dominant-active STAT that
1035 promotes tumorigenesis in Drosophila. *Dev Biol* **344**, 621-36.
1036   **Fisher, K. H., Stec, W., Brown, S. and Zeidler, M. P.** (2016). Mechanisms of
1037 JAK/STAT pathway negative regulation by the short coreceptor Eye
1038 Transformer/Latran. *Mol Biol Cell* **27**, 434-41.
1039   **Flaherty, M. S., Zavadil, J., Ekas, L. A. and Bach, E. A.** (2009). Genome-
1040 wide expression profiling in the Drosophila eye reveals unexpected repression of
1041 notch signaling by the JAK/STAT pathway. *Dev Dyn* **238**, 2235-53.
1042   **German, C. L., Sauer, B. M. and Howe, C. L.** (2011). The STAT3 beacon:
1043 IL-6 recurrently activates STAT 3 from endosomal structures. *Exp Cell Res* **317**,
1044 1955-69.
1045   **Gronholm, J., Ungureanu, D., Vanhatupa, S., Ramet, M. and**
1046 **Silvennoinen, O.** (2010). Sumoylation of Drosophila transcription factor STAT92E. *J*
1047 *Innate Immun* **2**, 618-24.
1048   **Guschin, D. Y., Waite, A. J., Katibah, G. E., Miller, J. C., Holmes, M. C.**
1049 **and Rebar, E. J.** (2010). A rapid and general assay for monitoring endogenous gene
1050 modification. *Methods Mol Biol* **649**, 247-56.
1051   **Henne, W. M., Stenmark, H. and Emr, S. D.** (2013). Molecular mechanisms
1052 of the membrane sculpting ESCRT pathway. *Cold Spring Harb Perspect Biol* **5**.
1053   **Horn, T., Sandmann, T. and Boutros, M.** (2010). Design and evaluation of
1054 genome-wide libraries for RNA interference screens. *Genome Biol* **11**, R61.
1055   **Hou, X. S., Melnick, M. B. and Perrimon, N.** (1996). Marelle acts
1056 downstream of the Drosophila HOP/JAK kinase and encodes a protein similar to the
1057 mammalian STATs. *Cell* **84**, 411-9.
1058   **Karsten, P., Hader, S. and Zeidler, M. P.** (2002). Cloning and expression of
1059 Drosophila SOCS36E and its potential regulation by the JAK/STAT pathway. *Mech*
1060 *Dev* **117**, 343-6.
1061   **Karsten, P., Plischke, I., Perrimon, N. and Zeidler, M. P.** (2006). Mutational
1062 analysis reveals separable DNA binding and trans-activation of Drosophila
1063 STAT92E. *Cell Signal* **18**, 819-29.
1064   **Kelly, B. T., McCoy, A. J., Spate, K., Miller, S. E., Evans, P. R., Honing, S.**
1065 **and Owen, D. J.** (2008). A structural explanation for the binding of endocytic
1066 dileucine motifs by the AP2 complex. *Nature* **456**, 976-979.
1067   **Kermorgant, S. and Parker, P. J.** (2008). Receptor trafficking controls weak
1068 signal delivery: a strategy used by c-Met for STAT3 nuclear accumulation. *J Cell Biol*
1069 **182**, 855-63.
1070   **Lawrence, R. E., Fromm, S. A., Fu, Y., Yokom, A. L., Kim, D. J., Thelen, A.**
1071 **M., Young, L. N., Lim, C. Y., Samelson, A. J., Hurley, J. H. et al.** (2019). Structural
1072 mechanism of a Rag GTPase activation checkpoint by the lysosomal folliculin
1073 complex. *Science* **366**, 971-977.
1074   **Makki, R., Meister, M., Pennetier, D., Ubeda, J. M., Braun, A., Daburon,**
1075 **V., Krzemien, J., Bourbon, H. M., Zhou, R., Vincent, A. et al.** (2010). A short
1076 receptor downregulates JAK/STAT signalling to control the Drosophila cellular
1077 immune response. *PLoS Biol* **8**, e1000441.
1078   **Mao, X., Ren, Z., Parker, G. N., Sondermann, H., Pastorello, M. A., Wang,**
1079 **W., McMurray, J. S., Demeler, B., Darnell, J. E., Jr. and Chen, X.** (2005).
1080 Structural bases of unphosphorylated STAT1 association and receptor binding. *Mol*
1081 *Cell* **17**, 761-71.
1082   **Marchetti, M., Monier, M. N., Fradagrada, A., Mitchell, K., Baychelier, F.,**
1083 **Eid, P., Johannes, L. and Lamaze, C.** (2006). Stat-mediated signaling induced by
1084 type I and type II interferons (IFNs) is differentially controlled through lipid
1085 microdomain association and clathrin-dependent endocytosis of IFN receptors. *Mol*
1086 *Biol Cell* **17**, 2896-909.

1087   **Mayor, S., Parton, R. G. and Donaldson, J. G.** (2014). Clathrin-Independent
1088   Pathways of Endocytosis. *Cold Spring Harbor Perspectives in Biology* **6**.
1089   **McBride, K. M., McDonald, C. and Reich, N. C.** (2000). Nuclear export
1090   signal located within theDNA-binding domain of the STAT1transcription factor.
1091   *EMBO J* **19**, 6196-206.
1092   **Mettlen, M., Chen, P. H., Srinivasan, S., Danuser, G. and Schmid, S. L.**
1093   (2018). Regulation of Clathrin-Mediated Endocytosis. *Annu Rev Biochem* **87**, 871-
1094   896.
1095   **Moore, R., Pujol, M. G., Zhu, Z. and Smythe, E.** (2018). Interplay of
1096   Endocytosis and Growth Factor Receptor Signalling. *Prog Mol Subcell Biol* **57**, 181-
1097   202.
1098   **Müller, P., Boutros, M. and Zeidler, M. P.** (2008). Identification of JAK/STAT
1099   pathway regulators--insights from RNAi screens. *Semin Cell Dev Biol* **19**, 360-9.
1100   **O'Shea, J. J., Schwartz, D. M., Villarino, A. V., Gadina, M., McInnes, I. B.**
1101   **and Laurence, A.** (2015). The JAK-STAT pathway: impact on human disease and
1102   therapeutic intervention. *Annu Rev Med* **66**, 311-28.
1103   **Owen, D. J., Collins, B. M. and Evans, P. R.** (2004). Adaptors for clathrin
1104   coats: structure and function. *Annu Rev Cell Dev Biol* **20**, 153-91.
1105   **Pandey, A., Fernandez, M. M., Steen, H., Blagoev, B., Nielsen, M. M.,**
1106   **Roche, S., Mann, M. and Lodish, H. F.** (2000). Identification of a novel
1107   immunoreceptor tyrosine-based activation motif-containing molecule, STAM2, by
1108   mass spectrometry and its involvement in growth factor and cytokine receptor
1109   signaling pathways. *J Biol Chem* **275**, 38633-9.
1110   **Ren, W., Zhang, Y., Li, M., Wu, L., Wang, G., Baeg, G. H., You, J., Li, Z.**
1111   **and Lin, X.** (2015). Windpipe controls Drosophila intestinal homeostasis by
1112   regulating JAK/STAT pathway via promoting receptor endocytosis and lysosomal
1113   degradation. *PLoS Genet* **11**, e1005180.
1114   **Robinson, M. S.** (2004). Adaptable adaptors for coated vesicles. *Trends Cell*
1115   *Biol* **14**, 167-74.
1116   **Schindler, C., Shuai, K., Prezioso, V. R. and Darnell, J. E., Jr.** (1992).
1117   Interferon-dependent tyrosine phosphorylation of a latent cytoplasmic transcription
1118   factor. *Science* **257**, 809-13.
1119   **Seibel, N. M., Eljouni, J., Nalaskowski, M. M. and Hampe, W.** (2007).
1120   Nuclear localization of enhanced green fluorescent protein homomultimers. *Anal*
1121   *Biochem* **368**, 95-9.
1122   **Shi, S., Larson, K., Guo, D., Lim, S. J., Dutta, P., Yan, S. J. and Li, W. X.**
1123   (2008). Drosophila STAT is required for directly maintaining HP1 localization and
1124   heterochromatin stability. *Nat Cell Biol* **10**, 489-96.
1125   **Shimizu, H., Woodcock, S. A., Wilkin, M. B., Trubenova, B., Monk, N. A.**
1126   **and Baron, M.** (2014). Compensatory flux changes within an endocytic trafficking
1127   network maintain thermal robustness of Notch signaling. *Cell* **157**, 1160-74.
1128   **Sigismund, S., Algisi, V., Nappo, G., Conte, A., Pascolutti, R., Cuomo, A.,**
1129   **Bonaldi, T., Argenzio, E., Verhoef, L. G., Maspero, E. et al.** (2013). Threshold-
1130   controlled ubiquitination of the EGFR directs receptor fate. *EMBO J* **32**, 2140-57.
1131   **Sigismund, S. and Scita, G.** (2018). The 'endocytic matrix reloaded' and its
1132   impact on the plasticity of migratory strategies. *Curr Opin Cell Biol* **54**, 9-17.
1133   **Sigismund, S., Woelk, T., Puri, C., Maspero, E., Tacchetti, C., Transidico,**
1134   **P., Di Fiore, P. P. and Polo, S.** (2005). Clathrin-independent endocytosis of
1135   ubiquitinated cargos. *Proc Natl Acad Sci U S A* **102**, 2760-5.
1136   **Silver, D. L., Geisbrecht, E. R. and Montell, D. J.** (2005). Requirement for
1137   JAK/STAT signaling throughout border cell migration in Drosophila. *Development*
1138   **132**, 3483-92.
1139   **Sousa, L. P., Lax, I., Shen, H., Ferguson, S. M., De Camilli, P. and**
1140   **Schlessinger, J.** (2012). Suppression of EGFR endocytosis by dynamin depletion

reveals that EGFR signaling occurs primarily at the plasma membrane. *Proc Natl Acad Sci U S A* **109**, 4419-24.

      Stahl, N. and Yancopoulos, G. D. (1994). The tripartite CNTF receptor complex: activation and signaling involves components shared with other cytokines. *J Neurobiol* **25**, 1454-66.

      Stark, G. R. and Darnell, J. E., Jr. (2012). The JAK-STAT pathway at twenty. *Immunity* **36**, 503-14.

      Stec, W., Vidal, O. and Zeidler, M. P. (2013). Drosophila SOCS36E negatively regulates JAK/STAT pathway signaling via two separable mechanisms. *Mol Biol Cell* **24**, 3000-9.

      Takeshita, T., Arita, T., Higuchi, M., Asao, H., Endo, K., Kuroda, H., Tanaka, N., Murata, K., Ishii, N. and Sugamura, K. (1997). STAM, signal transducing adaptor molecule, is associated with Janus kinases and involved in signaling for cell growth and c-myc induction. *Immunity* **6**, 449-57.

      Teis, D., Wunderlich, W. and Huber, L. A. (2002). Localization of the MP1-MAPK scaffold complex to endosomes is mediated by p14 and required for signal transduction. *Dev Cell* **3**, 803-14.

      Thiel, S., Dahmen, H., Martens, A., Muller-Newen, G., Schaper, F., Heinrich, P. C. and Graeve, L. (1998). Constitutive internalization and association with adaptor protein-2 of the interleukin-6 signal transducer gp130. *FEBS Lett* **441**, 231-4.

      Tognon, E., Wollscheid, N., Cortese, K., Tacchetti, C. and Vaccari, T. (2014). ESCRT-0 is not required for ectopic Notch activation and tumor suppression in Drosophila. *PLoS One* **9**, e93987.

      Traub, L. M. (2003). Sorting it out: AP-2 and alternate clathrin adaptors in endocytic cargo selection. *J Cell Biol* **163**, 203-8.

      Vander Ark, A., Cao, J. and Li, X. (2018). TGF-beta receptors: In and beyond TGF-beta signaling. *Cell Signal* **52**, 112-120.

      Vidal, O. M., Stec, W., Bausek, N., Smythe, E. and Zeidler, M. P. (2010). Negative regulation of Drosophila JAK-STAT signalling by endocytic trafficking. *J Cell Sci* **123**, 3457-66.

      Vieira, A. V., Lamaze, C. and Schmid, S. L. (1996). Control of egf receptor signaling by clathrin-mediated endocytosis. *Science* **274**, 2086-2089.

      Vietri, M., Radulovic, M. and Stenmark, H. (2019). The many functions of ESCRTs. *Nat Rev Mol Cell Biol*.

      Villarino, A. V., Kanno, Y. and O'Shea, J. J. (2017). Mechanisms and consequences of Jak-STAT signaling in the immune system. *Nat Immunol* **18**, 374-384.

      Villasenor, R., Kalaidzidis, Y. and Zerial, M. (2016). Signal processing by the endosomal system. *Curr Opin Cell Biol* **39**, 53-60.
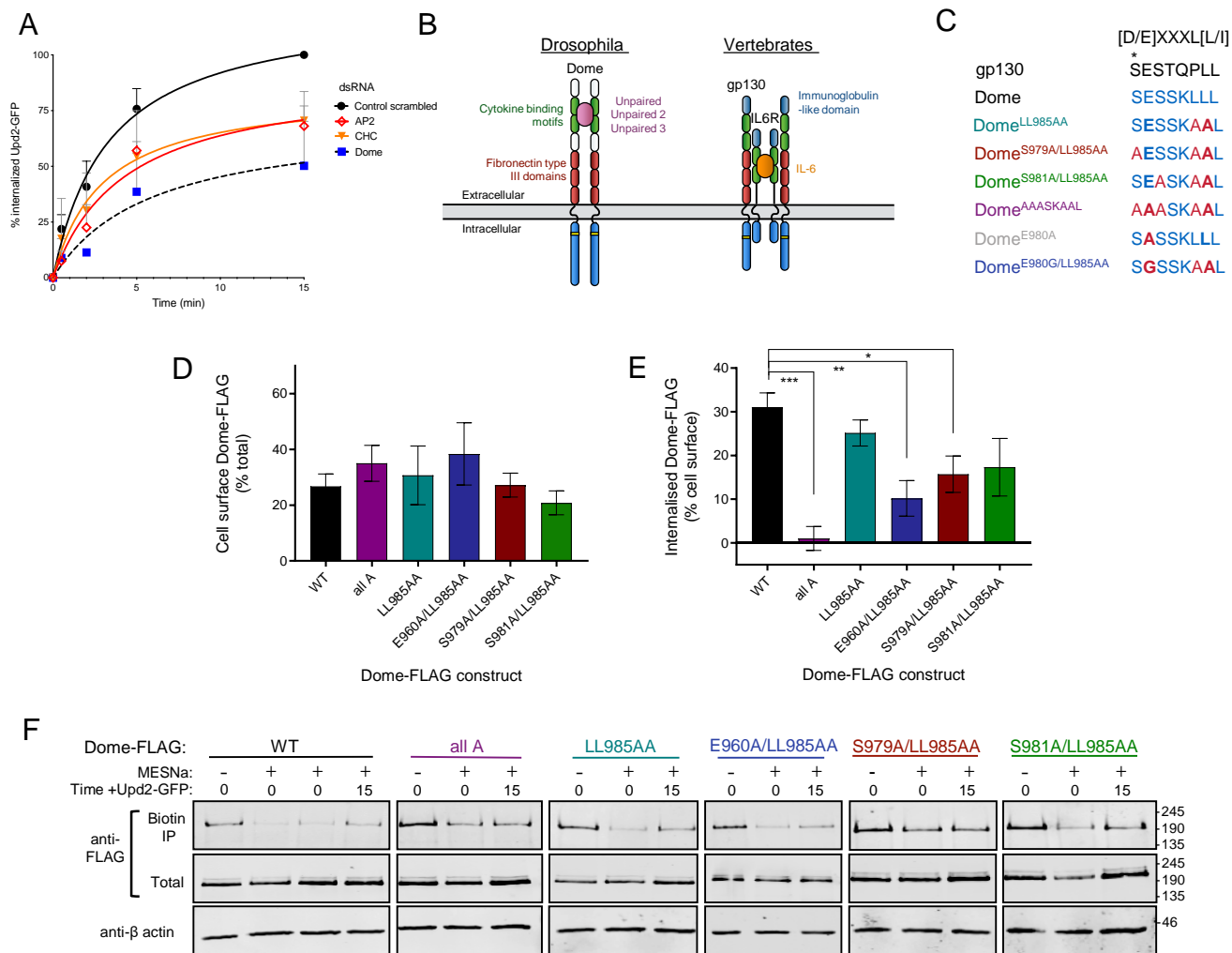
      Villasenor, R., Nonaka, H., Del Conte-Zerial, P., Kalaidzidis, Y. and Zerial, M. (2015). Regulation of EGFR signal transduction by analogue-to-digital conversion in endosomes. *Elife* **4**.
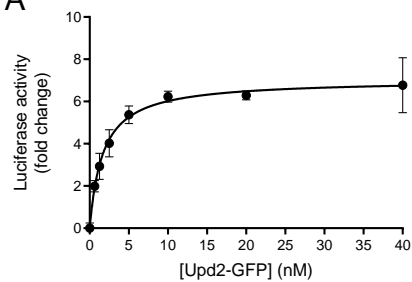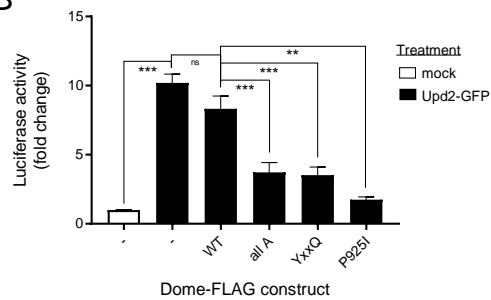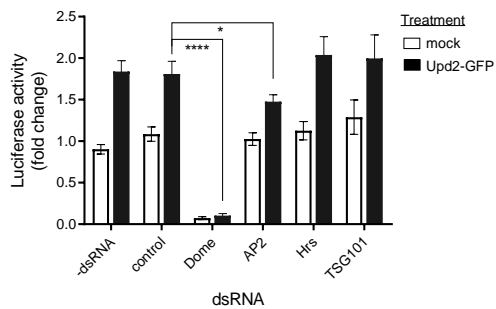
      Wang, R., Cherukuri, P. and Luo, J. (2005). Activation of Stat3 sequence-specific DNA binding and transcription by p300/CREB-binding protein-mediated acetylation. *J Biol Chem* **280**, 11528-34.

      Waterhouse, A., Bertoni, M., Bienert, S., Studer, G., Tauriello, G., Gumienny, R., Heer, F. T., de Beer, T. A. P., Rempfer, C., Bordoli, L. et al. (2018). SWISS-MODEL: homology modelling of protein structures and complexes. *Nucleic Acids Res* **46**, W296-W303.

      Weinberg, Z. Y. and Puthenveedu, M. A. (2019). Regulation of G protein-coupled receptor signaling by plasma membrane organization and endocytosis. *Traffic* **20**, 121-129.

1195   **Wenta, N., Strauss, H., Meyer, S. and Vinkemeier, U.** (2008). Tyrosine
1196 phosphorylation regulates the partitioning of STAT1 between different dimer
1197 conformations. *Proc Natl Acad Sci U S A* **105**, 9238-43.
1198   **Wright, V. M., Vogt, K. L., Smythe, E. and Zeidler, M. P.** (2011). Differential
1199 activities of the Drosophila JAK/STAT pathway ligands Upd, Upd2 and Upd3. *Cell*
1200 *Signal* **23**, 920-7.
1201   **Yan, R., Small, S., Desplan, C., Dearolf, C. R. and Darnell, J. E., Jr.**
1202 (1996). Identification of a Stat gene that functions in Drosophila development. *Cell*
1203 **84**, 421-30.
1204   **Zeidler, M. P. and Bausek, N.** (2013). The Drosophila JAK-STAT pathway.
1205 *JAKSTAT* **2**, e25353.
1206

A

% internalized Upd2-GFP vs Time (min)

dsRNA:
- Control scrambled
- AP2
- CHC
- Dome

B

Drosophila

Dome
- Cytokine binding motifs
- Unpaired
- Unpaired 2
- Unpaired 3
- Fibronectin type III domains
- Extracellular
- Intracellular

Vertebrates

gp130
- IL6R
- IL-6
- Immunoglobulin-like domain

C

[D/E]XXXL[L/I]

gp130   SESTQPLL
Dome   SESSKLLL
Dome^LL985AA   SESSKAAL
Dome^S979A/LL985AA   AESSKAAL
Dome^S981A/LL985AA   SEASKAAL
Dome^AAASKAAL   AAASKAAL
Dome^E980A   SASSKLLL
Dome^E980G/LL985AA   SGSSKAAL

D

Cell surface Dome-FLAG (% total) vs Dome-FLAG construct

WT, all A, LL985AA, E960A/LL985AA, S979A/LL985AA, S981A/LL985AA

E

Internalised Dome-FLAG (% cell surface) vs Dome-FLAG construct

WT, all A, LL985AA, E960A/LL985AA, S979A/LL985AA, S981A/LL985AA

*** ** *

F

Dome-FLAG: WT | all A | LL985AA | E960A/LL985AA | S979A/LL985AA | S981A/LL985AA
MESNa: − + + + | − + + + | − + + + | − + + + | − + + + | − + + +
Time +Upd2-GFP: 0 0 0 15 | 0 0 0 15 | 0 0 0 15 | 0 0 0 15 | 0 0 0 15 | 0 0 0 15

anti-FLAG
- Biotin IP — 245, 190, 135
- Total — 245, 190, 135

anti-β actin — 46

A

[Upd2-GFP] (nM) : 0   25   12.5   6.25   3.13   1.53   0.77   0.38   0.19   0.1

p-STAT92E →
STAT92E →
                                                                    80kDa

B

Phosphorylated STAT92E (% total STAT92E)

60

40

20

0

[Upd2-GFP] (nM)

0 1 2 3 4 5   5 10 15 20 25

C

CIP   -   -   +
Upd2-GFP   -   +   +

p-STAT92E →
STAT92E →
                        80kDa

D

Phosphorylated STAT92E (% total STAT92E)

60

40

20

Mock   Upd2-GFP   Upd2-GFP + CIP

Treatment

E

dsRNA
☐ Control
■ AP2

Phosphorylated STAT92E (% total STAT92E)

60

40

20

0

0   5   10   15

Time (mins)

F

Time (mins)   Control dsRNA   AP2 dsRNA
+ Upd2-GFP : 0   2   5   10   15   0   2   5   10   15

p-STAT92E →
STAT92E →
                                                          80kDa

G

Phosphorylated Tyrosine^{704} Mod/Base ratio

1.0

0.8

0.6

0.4

0.2

0.0

dSRNA   Control   Control   AP2
Upd2-GFP   -   +   +

A

[Upd2-GFP] (nM) :   0   25   12.5 6.25 3.13 1.53 0.77 0.38 0.19   0.1

p-STAT92E →
STAT92E →   80kDa

B

| CIP | − | − | + |
| Upd2-GFP | − | + | + |

p-STAT92E →
STAT92E →   80kDa

C

D

dsRNA
☐ Control
■ AP2

E

Time (mins)   Control dsRNA   AP2 dsRNA
+ Upd2-GFP :   0   2   5   10   15   0   2   5   10   15

p-STAT92E →
STAT92E →   80kDa

F

G

(f)

A

[Upd2-GFP] (nM) : 0 25 12.5 6.25 3.13 1.53 0.77 0.38 0.19 0.1

p-STAT92E →
STAT92E →
80kDa

B

Phosphorylated STAT92E
(% total STAT92E)

60

40

20

0

0 1 2 3 4 5 7 10 15 20 25
[Upd2-GFP] (nM)

C

D

CIP   -   -   +
Upd2-GFP   -   +   +

p-STAT92E →
STAT92E →
80kDa

Phosphorylated STAT92E
(% total STAT92E)

60

40

20

0

Mock   Upd2-GFP   Upd2-GFP
                      + CIP
Treatment

Time (mins)   Control dsRNA   AP2 dsRNA
+ Upd2-GFP : 0   2   5   10   15   0   2   5   10   15

p-STAT92E →
STAT92E →
80kDa

Phosphorylated STAT92E
(% total STAT92E)

60

40

20

0

dsRNA
□ Control
■ AP2

0   5   10   15
Time (mins)

E

Phosphorylated Tyrosine^704
Mod/Base ratio

0.8

0.6

0.4

0.2

0.0

Control   Control   AP2

F

(f)

A

dsRNA

Control   Dome   AP2   Hrs

Time (mins) + 3nM Upd2-GFP

0

30

B

Nuclear/ cytoplasmic STAT92E-GFP (normalised to 30min)

Time (mins)

C

Nuclear/ cytoplasmic STAT92E-GFP (normalised to control 0min)

****

ns

STAT-GFP mutant
■ STAT^WT-GFP
■ STAT^Y704F-GFP

Time (mins) + Upd2-GFP

0   15   30

D

Nuclear/ cytoplasmic STAT92E-GFP (normalised to control 0min)

****   ****   ns   ns

Time (mins) + Upd2-GFP
□ mock
■ Upd2-GFP

control   Dome   AP2   Hrs

dsRNA

A

Time (mins) + 3nM Upd2-GFP

0   15   30

STAT92E-GFP construct

WT

T702V

B

Nuclear/ cytoplasmic STAT92E-GFP (normalised to control 0min)

****

ns

STAT-GFP mutant
STAT92E^{WT}-GFP
STAT92E^{T702V}-GFP

Time (mins) + Upd2-GFP

C

Phosphorylation of Tyrosine^{704} Mod/Base ratio

STAT92E-GFP construct: WT   WT   T702V
Upd2-GFP: -   -   +

D

CCP

CCV

EE

LE/MVB

Nucleus

Upd2/Dome
Clathrin coated pit/vesicle (CCP/V) containing AP2
Ubiquitin
Hrs
TSG101

E

(i)

STAT92E-C $_{697}$RQDPVTGYVKSTLHV$_{711}$
STAT92E-F $_{704}$VLDPVTGYVKSTLHV$_{718}$
hSTAT1 $_{694}$DGPKGTGYIKTELIS$_{708}$
hSTAT5a $_{687}$LAKAVDGYVKPQIKQ$_{701}$
hSTAT5b $_{692}$TAKAADGYVKPQIKQ$_{706}$

(ii)

(iii)

Threonine   Tyrosine